ARL 69-0160
SEPTEMBER 1969

3

Aerospace Research Laboratories

EXPLORATORY EXPERIMENTS IN WATER ON STREAM-WISE VORTICES AND CROSSHATCHING OF THE SURFACE OF REENTRY BODIES

LIEF N. PERSEN
INSTITUTT FOR MEKANIKK
TRONDHEIM, NORWAY

Contract No. F33615-67-C-1758
Project No. 7063

OFFICE OF AEROSPACE RESEARCH
United States Air Force

81

NOTICES

When Government drawings, specifications, or other data are used for any purpose other than in connection with a definitely related Government procurement operation, the United States Government thereby incurs no responsibility nor any obligation whatsoever; and the fact that the Government may have formulated, furnished, or in any way supplied the said drawings, specifications, or other data, is not to be regarded by implication or otherwise as in any manner licensing the holder or any other person or corporation, or conveying any rights or permission to manufacture, use, or sell any patented invention that may in any way be related thereto.

Agencies of the Department of Defense, qualified contractors and other government agencies may obtain copies from the

Defense Documentation Center
Cameron Station
Alexandria, Virginia 22314

This document has been released to the

CLEARINGHOUSE
U.S. Department of Commerce
Springfield, Virginia 22151

for sale to the public.

Copies of ARL Technical Documentary Reports should not be returned to Aerospace Research Laboratories unless return is required by security considerations, contractual obligations or notices on a specified document.

400 - April 1970 - CO455 - 114-2513

ARL 69-0160

EXPLORATORY EXPERIMENTS IN WATER ON STREAM-WISE VORTICES AND CROSSHATCHING OF THE SURFACE OF REENTRY BODIES

LIEF N. PERSEN
INSTITUTT FOR MEKANIKK
TRONDHEIM, NORWAY

SEPTEMBER 1969

Contract No. F33615-67-C-1758
Project No. 7063

AEROSPACE RESEARCH LABORATORIES
OFFICE OF AEROSPACE RESEARCH
UNITED STATES AIR FORCE
WRIGHT-PATTERSON AIR FORCE BASE, OHIO

F O R E W O R D

The author spent his sabbatical leave at the Aerospace Research Laboratories at Wright-Patterson AFB in the period September 1968 - August 1969 with the objective of studying stream-wise directed vortex systems. The report describes in detail some of the reults obtained experimentally using the water jet as an experimental device. Information was in that way obtained on the stream-wise striations observed on ablating surfaces as well as on coated surfaces when exposed to boundary layer flow. Dr. Max Scherberg advanced the idea that the author's water jet experiments could be used to study the ablation process. This idea proved to be very fruitful, and consequently the results were divided into two parts which could be treated separately.

Apart from some observations closely related to the ablation process the present report is mainly concerned with the stream-wise vortices, their spacing and its relation to the outside flow and to the origin of these vortices. A second report will be prepared on the ablation process and a brief extract of it has already been submitted for publication.

Theoretical work on the subject has also been undertaken and a third report will give that part of the investigation.

A B S T R A C T

Contained in this report is a detailed description of the experimental results obtained on the stream-wise vortices using a water jet as an experimental device. Information on the vortices were obtained through a study of the stream-wise striations left in the coat on the models used by the outside flow. Striation counts were performed and the "wavenumber" thus obtained is related to the flow parameters. The contention that the stream-wise vortices appear as a result of the outside curved flow becoming unstable is strongly supported. The investigation is not finished and further work has already been undertaken.

T A B L E OF C O N T E N T S

LIST OF FIGURES

EXPLORATORY EXPERIMENTS IN WATER ON STREAM-WISE DIRECTED VORTICES AND CROSSHATCHING OF THE SURFACE OF REENTRY BODIES

by

Leif N. Persen

#1. Introduction.

In recent years the study of stream-wise directed vortices in fluid flows which usually are thought of as being two-dimensional or axis-symmetrical has attracted a widespred attention. A survey of a selected number of papers exhibiting experimental evidence of the existence of vortex systems of this type has been prepared by the author [1], and the present series of experiments is aimed at gaining more detailed information on these vortex systems. Lately the hypothesis has been advanced that these vortices are responsible for the initiation of the criss-cross pattern which occur under certain conditions on the surface of ablating objects such as reentry bodies. Although the study of ablation is not the main purpose of the present investigation, some of the observations made seem highly relevant to this phenomenon and are consequently reported on here.

The decision to use water as the working fluid was made because the author had observed patterns to occur in his kitchen sink which could be interpreted as stream-wise directed vortices being formed when the jet from the tap hit the bottom of the sink. Fig. 1 shows this observation as

Fig. 1

it occurred, and the "stream-wise vortices" are seen to go straight through the radial waves as well as through the hydraulic jump. The explanation for the "vortices" to be visible is sought in the difference between the light being reflected from the shiny bottom surface through a "vortex" and that being reflected between two "vortices".

To verify if the phenomenon observed really is caused by vortices the same technique was used as in other experiments of this type. A glass plate was given a coat of paint and was then exposed to the water jet from an ordinary faucet before the paint was dry. The result is shown in Fig. 2.

Fig. 2

The dark spots should be ignored because they indicate areas where the paint was washed away immediately due to remnants of the cleaning fluid which had been used. The striations in the coat are however clearly visible and as in other investigations this is interpreted as experimental evidence of the presence of stream-wise vortices in the flow.

Already at this point it should be mentioned why the notation "vortex" is put in quotation. By a vortex one usually envisages a flow where the path of a fluid particle takes the shape of a spiral as sketched in Fig. 3. The appearance of striations is then attributed to the "drilling" effect that the flow exerts on the coat with the shear stress as the acting force. This is also indicated in Fig. 3. One may however envisage a situation where the vortex is so weak that it can hardly be regarded as a vortex in the usual sense. It is rather to be regarded as a perturbation which however may cause a cross-wise fluctuation in the velocity profile for the velocity component of the main stream as sketched in Fig. 4. The striations are then formed because of the periodic variation in the stream-wise directed shear

stress. Also cases where these two effects are combined may occur. In all

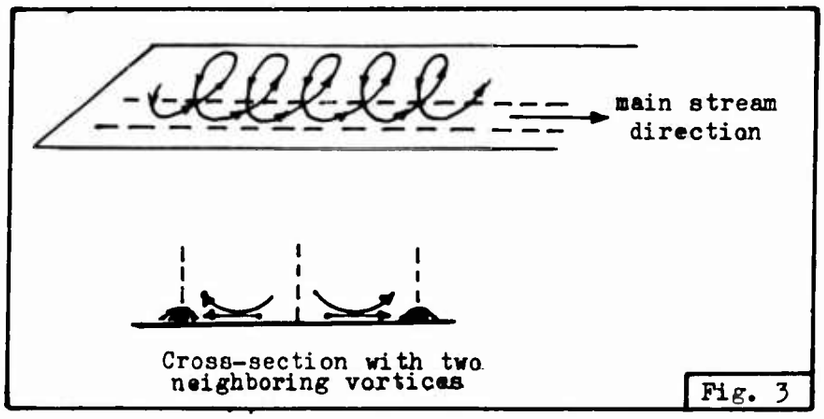

Fig. 3

cases where striations occur one shall here use the notation stream-wise vortices without regard to the physical mechanism which may be responsible for the formation of these striations.

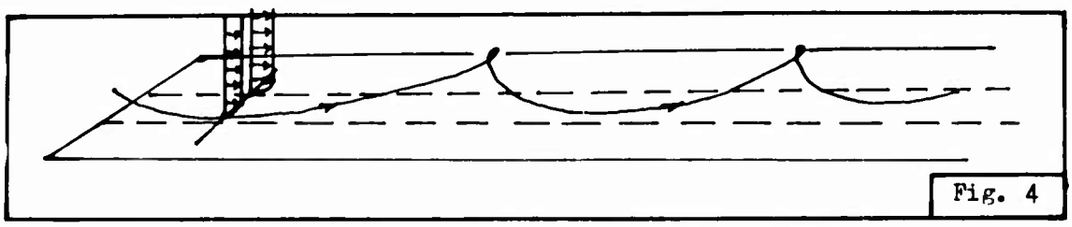
Fig. 4

#2. The experimental set-up.

The results given in the introductory remarks encouraged further exploratory experiments to be undertaken to see to what extent such experiments could give valuable information on systems of stream-wise directed vortices. For that purpose the experimental set-up sketched in Fig. 5 was built. It is rather simple and consists of an elevated tank from which a straight 2" pipe leads down to a nozzle (A). Three nozzles were used giving jets with a diameter of 1/8", 2/8" and 3/8". The tank contains an amount of water which is large compared with the amount used during each run. This enables a rather steady head to be kept during each experiment. The volume above the free water-surface in the tank can either be pressurized or evacuated whereby the velocity of the jet can be varied within a large range. Just above the nozzle is a manometer (B) reading the static pressure in the tube at that point. This is kept constant during each run through a bleeding valve (C) in the evacuation pipe.

In addition to this set-up a water table was used. A sketch illu-

strating the principle of this table is given in Fig.6. The water is being pumped from the lower tank (L) to the upper tank (U) from which it runs over a steep plate (A) on to a slightly inclined plate (B). From this it returns to the lower tank. The water table was used in an attempt to establish a plane flow which could be used for the purpose of comparison with the axis-symmetric cases studied with the water jet.

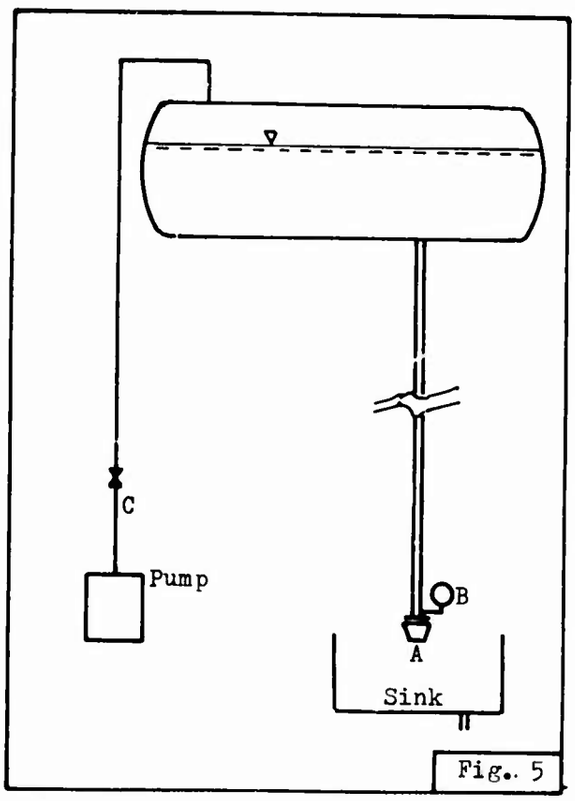

Fig. 5

The water table can not be used with paint coating because it has a closed water system, and ablated material would tend to clogg up this system. The number of experiments with the water table to be reported on here will consequently be rather limited.

Because a coating technique could not be used the two plates (A) and (B) were polished to a high shine in order to make observations of the same type as in the original kitchen sink experiment possible.

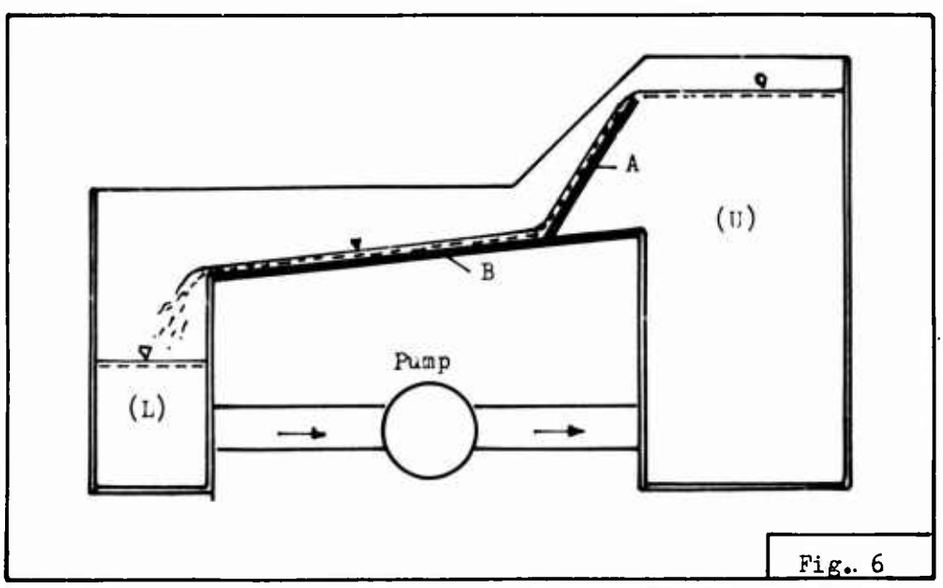

Fig. 6

#3. A qualitative experiment. Secondary flow.

A number of different coating materials were tried out to find one suited for exhibiting the effect of eventual vortices on the surface as well as showing ablation effects. Among others very fine-grained sand was used. This did not serve the purpose for which it was intended, but an effect that may be important in these experiments were brought to light. This effect will here be called secondary motion.

When the water jet hits the plate at right angle a stagnation flow will appear as sketched in Fig. 7. The hydraulic jump will be located at a distance from the line of symmetry which can be regulated by changing the amount of water discharged. With sand on the surface the sand is imme-

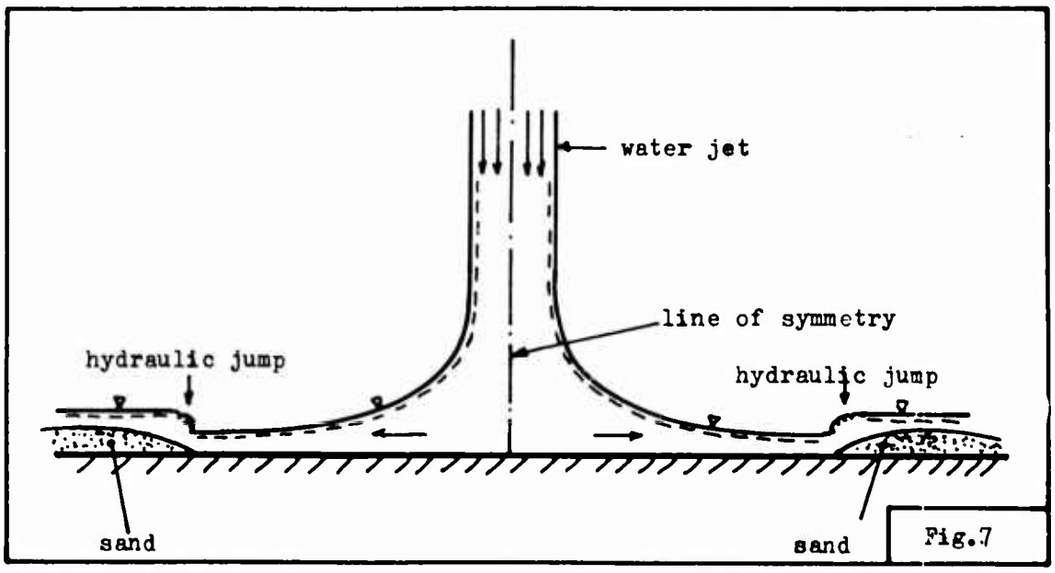

Fig.7

diately washed away inside the region bounded by the hydraulic jump. It gathers in a smooth ringshaped heap at the hydraulic jump as indicated in Fig. 7. Fig. 8 shows a picture of this situation as it occurred under the jet from an ordinary faucet. It should be noted that circular waves will occur in the inner region and that the light reflected from these waves is broken up at regular intervals. This is indicative of the presence of streamwise directed vortices in the flow.

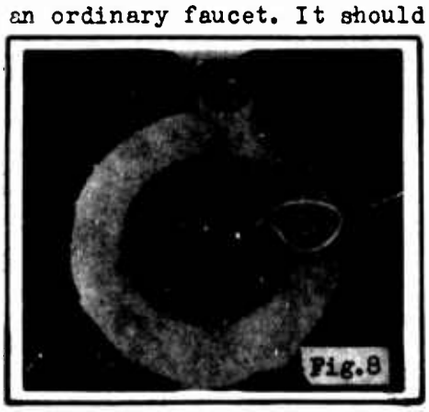
Fig.8

If now the discharge of water is regulated down slightly, the hydraulic jump will occur on a circle with a smaller radius and an interesting phenomenon takes place. Apparently due to the presence of the stream-

wise vortices sand is extracted inwards from the sand bank in stripes as exhibited in Fig.9a. Only seconds later the extracted sand will gather in heaps regularly spaced around the circle where the hydraulic jump occurs. This is shown in Fig.9b which is taken less than 10 sec. after Fig. 9a. No quantitative measurements were made, but there seemed to be no apparent relation between the frequency of the vortex system and the number of heaps. To investigate this phenomenon closer, a film was made of the pro-

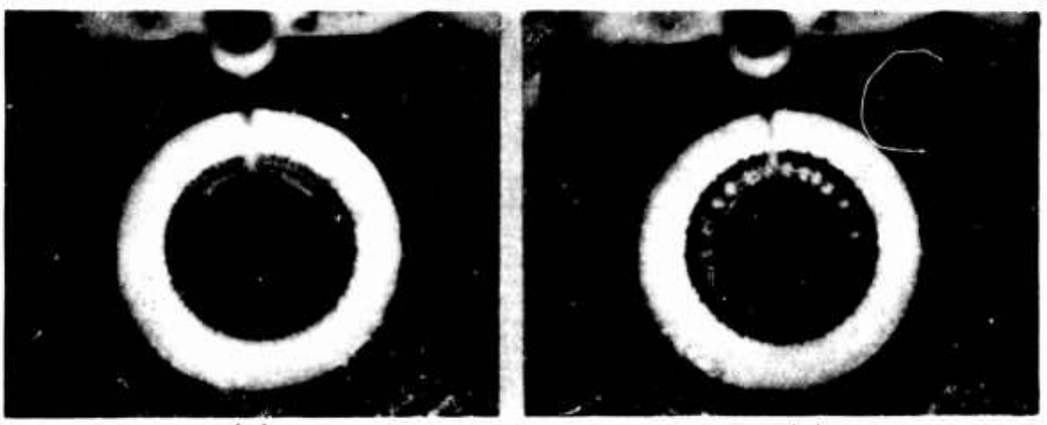

(a) (b)

Fig.9

cess.Fig.10 shows a series of frames reproduced from that film which clearly brings out the fact that the number of heaps formed at the new location of the hydraulic jump is not constant. The number of heaps decreases with time, and this apparently is achieved by two neighboring heaps merging into one. An explanation for this can be found in the existence of secondary flow. It is known that when a frequency (such as the frequency of the stream-wise vortices) is introduced into the flow of a fluid, the non-linearity of the Navier-Stokes' equations will give rise to higher order frequencies and secondary flow. (streaming). The slowly varying pattern in the sand may be thought of as such streaming. Apart from the basic interest the visualization of secondary flow may have, the result has a bearing on the experiments to be reported on here. In the present case the sand serves the purpose of making the flow visible. Thus if one stopped the experiment at a certain stage and observed the heaps only, one could be led to believe that their spacing is representative of a corresponding regular periodicity in the flow. It is clearly brought out that this is not so.

In performing experiments with the basic idea of gathering information about the flow from marks made by the fluid on a coating material

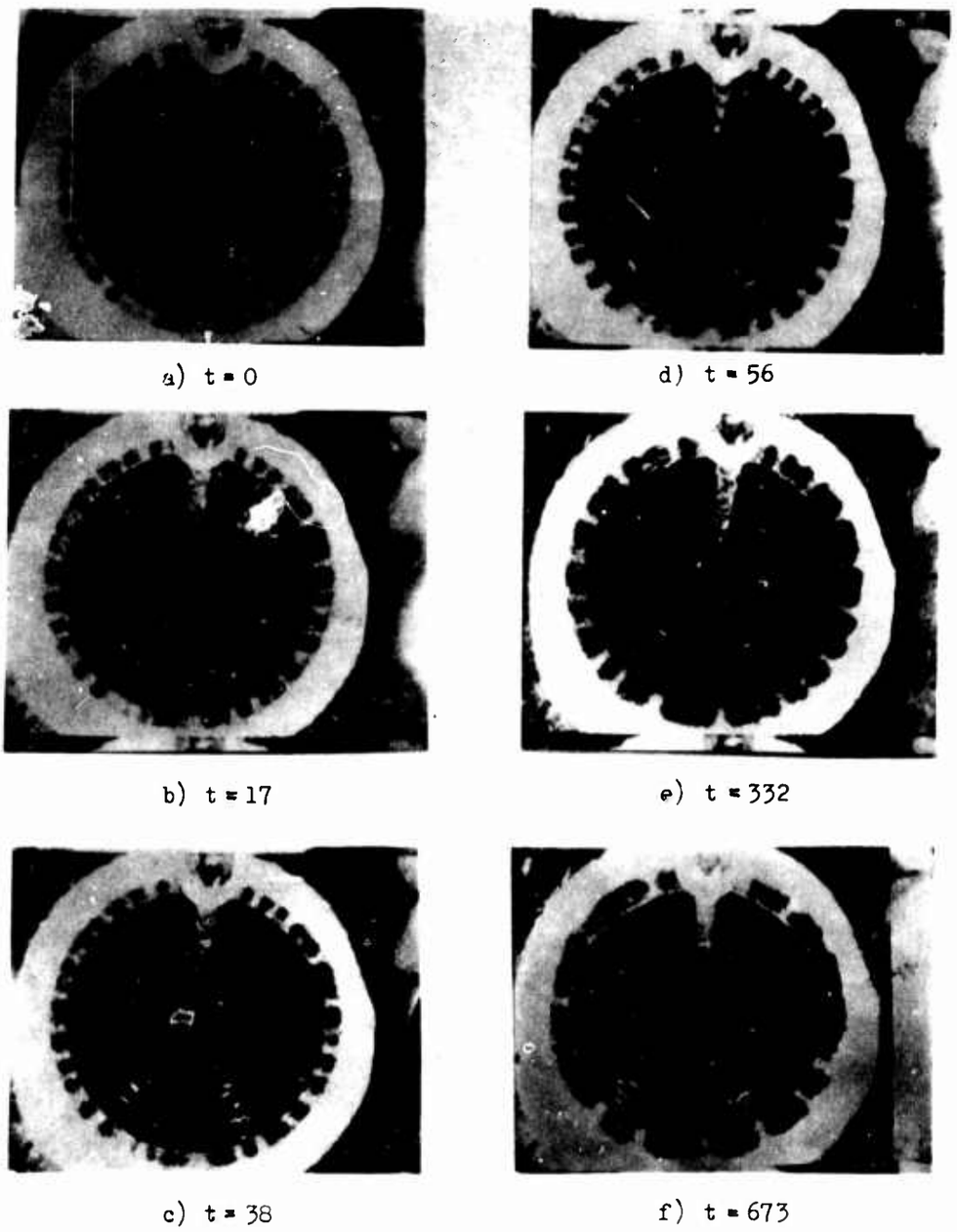

a) t = 0

d) t = 56

b) t = 17

e) t = 332

c) t = 38

f) t = 673

Fig.10 Sequence taken from film showing secondary flow visualized by loose sand on a plate exposed to a water jet. The time t is given in 1/24 sec. Total time of sequence: 28 1/24 sec.

one should therefore bear in mind the possibility of time-effects. Usually this is taken care of by extending the running time in each case sufficiently to make sure that the pattern is not depending on the duration of the run.

#4. Some selected papers on "cross-hatching".

Before proceding to report on the experimental results which may be relevant in the "cross-hatching" process it seems appropriate to give a short reference to a few recent papers concerned with this phenomenon. H.K.Larson and G.G.Mateer [3] describes it as follows: "Ablation patterns have been observed on recovered flight objects, ballistic range models and wind tunnel models. These patterns result from orderly, criss-crossed grooves to relatively disordered gouges similar to regmaglypt surface features on meteorites." The three papers to be considered here are all aimed at understanding the process responsible for the criss-cross patterns mentioned above.

The paper by T.N.Canning, M.E.Tauber, M.E.Wilkins and G.T.Chapman [4] fixes its main attention on the fact that the regular pattern is found in regions where the boundary layer is turbulent and where consequently one would not expect any regularity to occur. Several models of different shapes were used and tested in a wind tunnel. They were inserted into the stream after steady flow was established and withdrawn from the stream after an interval which was determined **optically** during the run in each case. Only the one model shown in Fig.11 will be drawn to attention here. The criss-cross pattern on the cone below the point where the cone-angle changes abrubtly is clearly visible. It seems to be the firm belief of the authors that a close connection between the cross-hatching process and the stream-wise vortices is present.

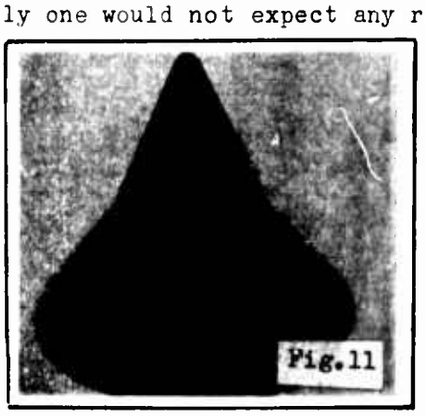
Fig.11

In [3] a series of tests is reported on, and several observations will be drawn to attention here. First it is noticed that the cross-hatched pattern does not seem to be time-independant. A longtime change in the pattern is observed similar to the longtime change discussed in Sec. #3. It should be stressed however that the physical interpretations are quite different in the two cases. Next it is noticed that on most models "stream-wise grooves were present in the region between the tip and the beginning of cross-hatching." Fig.12 and Fig.13 are reproduced from [3]. Fig. 12a shows a typical cross-hatched pattern obtained when the surface Mach number is greater than

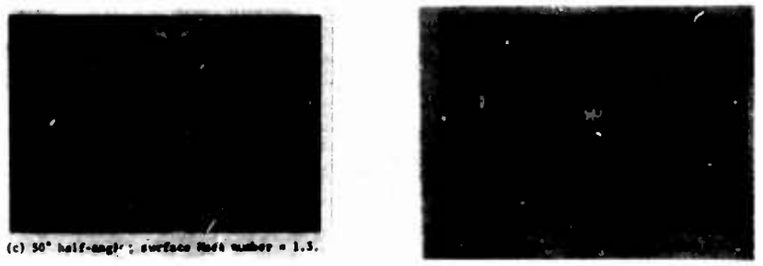

(a) (b)

Fig.12

one. Fig.12b shows a wavy pattern (no cross-hatching) when the surface Mach number is less than one. Fig.13 shows the ablation of a cone at three different stages, i.e. after 1, 2 and 3 secs exposure to the stream. Both in [3] and [4] the models are made of a material that will ablate when exposed to the stream. In the experiments to be reported on here the ablation process is to be simulated with paint used as a coating. Some striking similarities with the findings shown here will be presented later.

Fig. 13

M.Tobak [2] has presented a hypothesis for the origin of cross-hatching. In his presentation the presense of a "stationary array of longitudinal vortices" is a prerequisite for the theory. The origin of these vortices is given as "small irregularities in the surface at or near the leading edge". The present investigation indicates however that the vortices appear as a result of instability of the main flow as is emphasized later. Also the general consept of the mechanism leading to cross-hatching is different from the results obtained by the present author to be reported on elsewhere. However, the importance of the stream-wise directed vortices in this connection seems well established.

From the rather brief exposition given here it is natural to try to gain more information on the stream-wise directed vortices.

#5. Qualitative results on a sphere.

The first experiments performed with the water-jet apparatus described in Sec.#2 used a sphere as a model. The sphere was coated with paint using a spray-can. The paint had an oil base to prevent it from mixing with the water. It turned out that the drying time (i.e. the time between application of the paint and the exposure of the model to the stream) was essential to the success of the experiment. If the drying time was too long the energy in the jet turned out to be insufficient to make any impression on the coat. If it was too short many features of the process that took place were "washed away" without being properly recognized. Also the thickness of the coat had to be kept within certain limits for the same reason.

A film was prepared of the process that took place and Fig. 14 and Fig. 15 are reproductions of selected frames from this film. It should be stressed that in this case the paint had been allowed to dry so long that the smooth flow of water over the surface had no appreciable effect on the coat. It is therefore remarkable to notice that under these conditions a phenomenon took place whereby impressions in the coat (like scratchings with a sharp instrument) were made in areas where local separation occurred. Fig.13a represents an attempt to sketch the process.

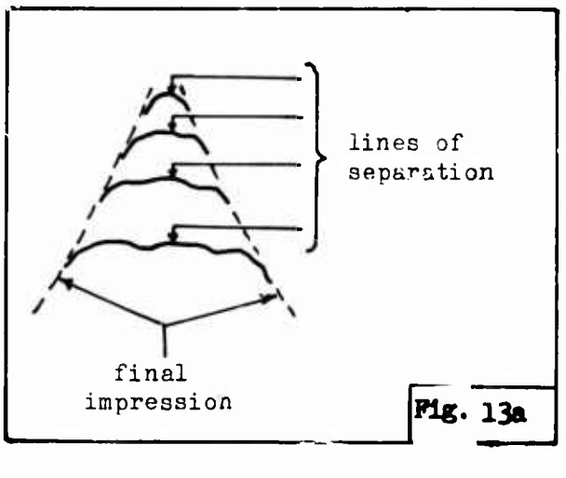

Fig. 13a

At the equator of the sphere local separation would occur at a point. From this point a triangularly shaped area of the sphere would not be wetted by water. The point of separation would move downstreams (as a tidal wave moving ashore) as indicated by the "lines of separation" in Fig.16. The flow will finally be reattached and the coat will have received a sharp impression as indicated in Fig. 16. Because this process takes place at different starting points a criss-cross pattern will appear around the equator of the sphere. Figs. 14 and 15 show two examples of this process and the frames a) indicate with an arrow where the process starts. A comparison between a) and

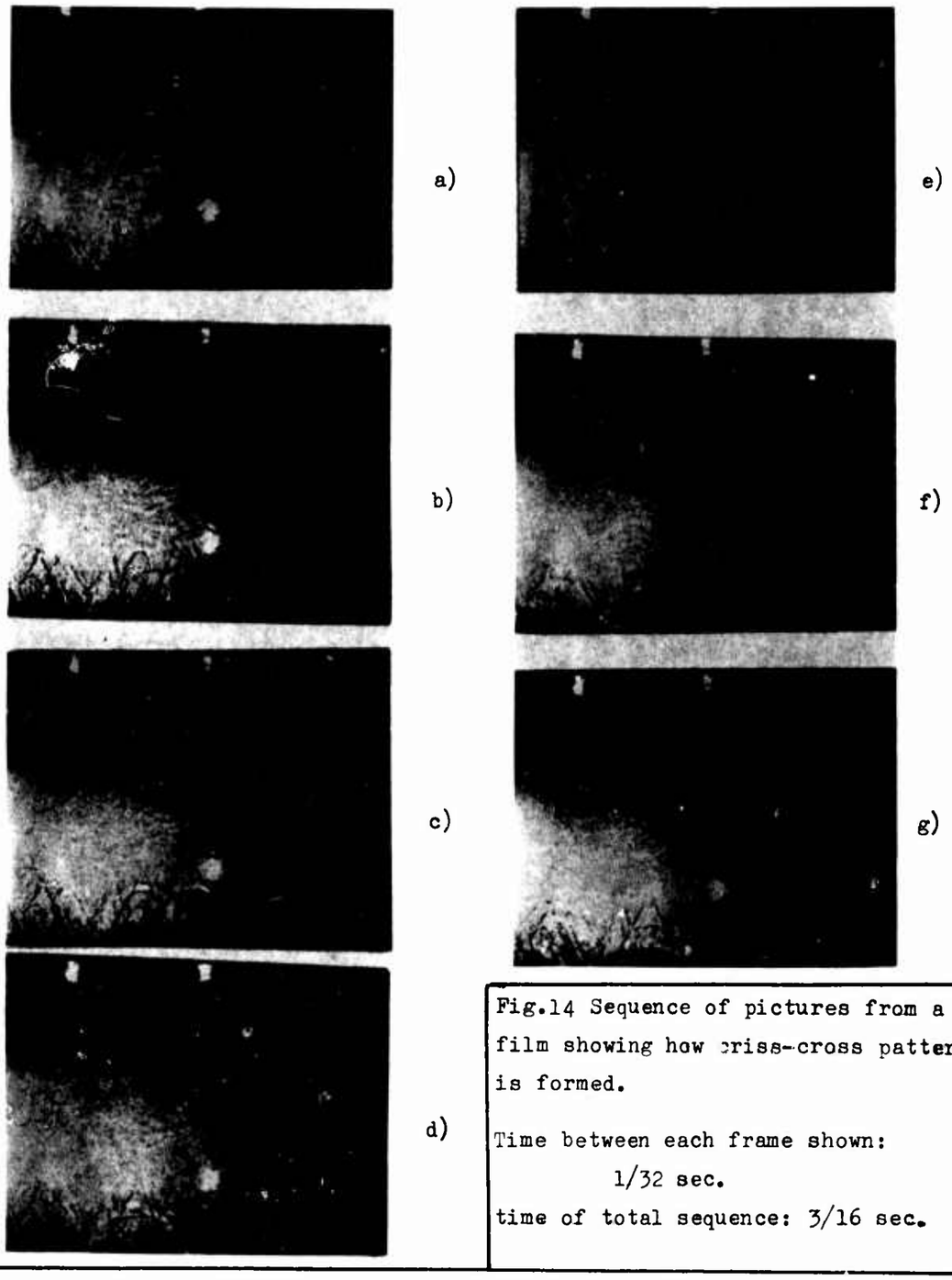

Fig.14 Sequence of pictures from a film showing how criss-cross pattern is formed.

Time between each frame shown:
1/32 sec.
time of total sequence: 3/16 sec.

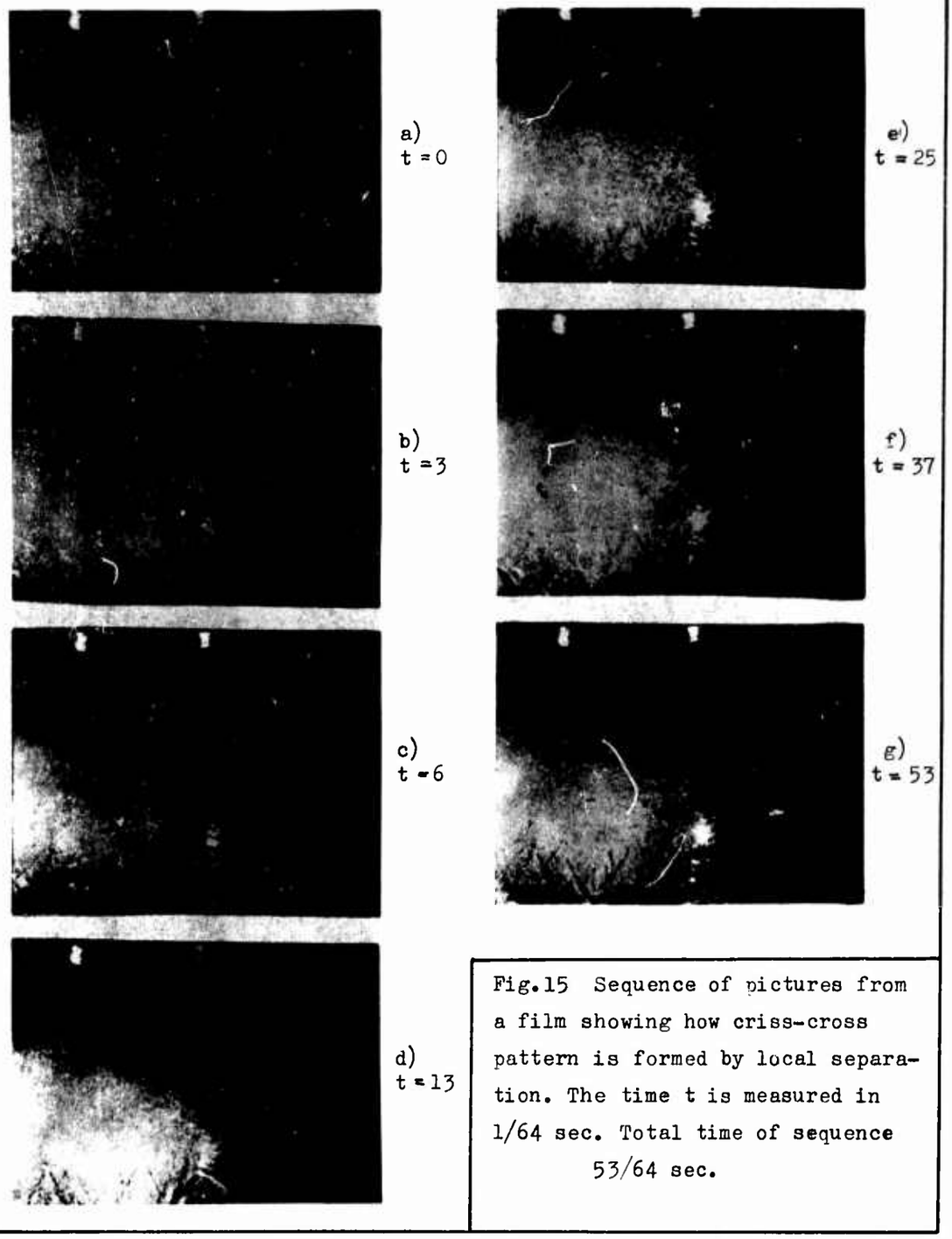

Fig.15 Sequence of pictures from a film showing how criss-cross pattern is formed by local separation. The time t is measured in 1/64 sec. Total time of sequence 53/64 sec.

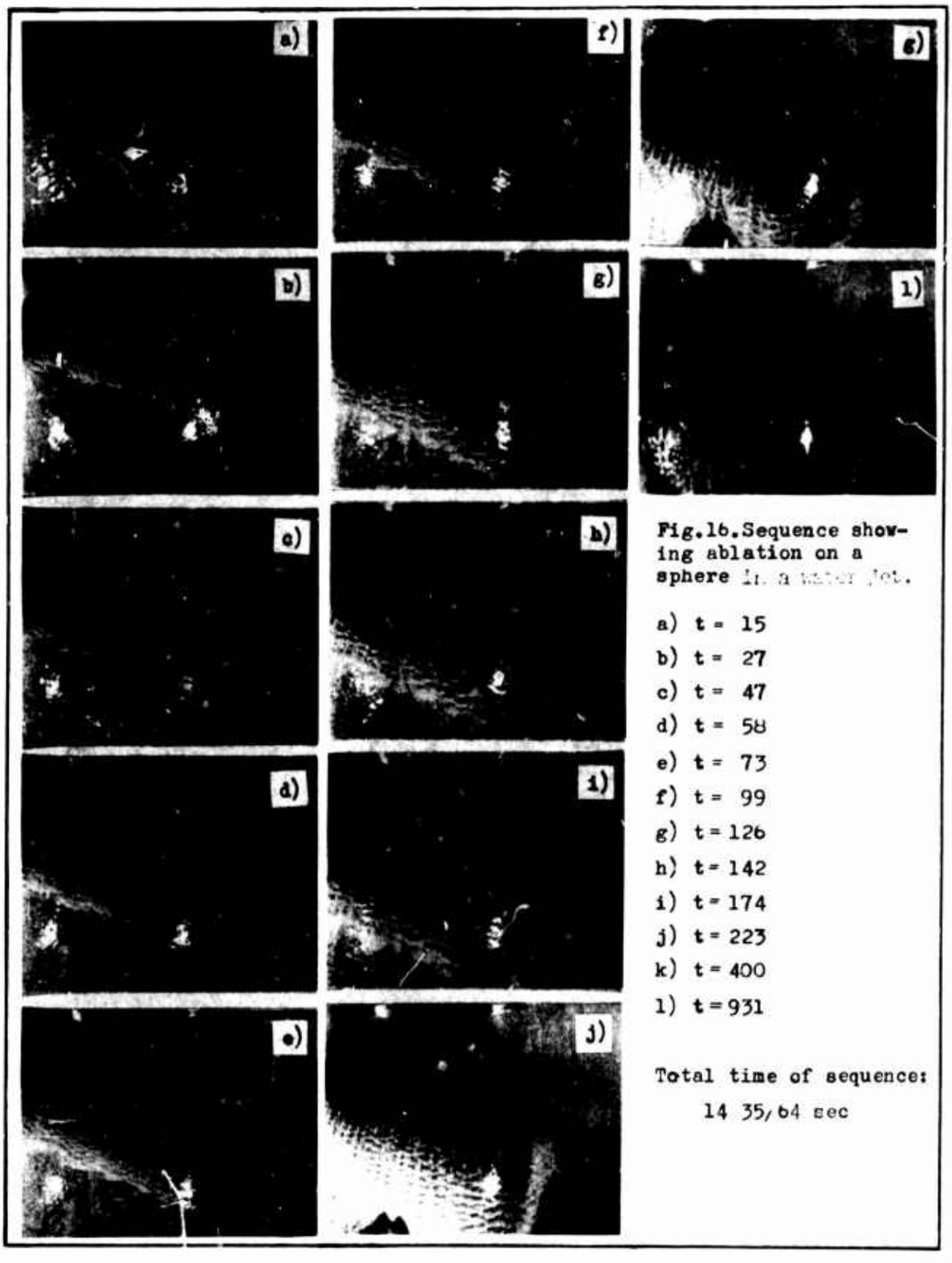

Fig.16.Sequence showing ablation on a sphere in a water jet.

a) t = 15
b) t = 27
c) t = 47
d) t = 58
e) t = 73
f) t = 99
g) t = 126
h) t = 142
i) t = 174
j) t = 223
k) t = 400
l) t = 931

Total time of sequence:
14 35/64 sec

g) in each sequence shows the trace having been made where none existed before. The sequence in Fig.14 is much shorter than in Fig. 15 and consequently the trace left is much more pronounced in the latter case.

The remarkable feature of this observation is that apparently very strong forces (compared with the forces exerted by the flow elsewhere on the coat) are acting on the coat at the separation envelope to give traces in the coat which elsewhere seems to be unaffected by the flow.

Fig. 16 shows a sequence of the film taken from a run where the paint was given a much shorter drying time. The times t given in the sequence is counted in 1/64 secs. In the frames a)-d) a wavy pattern similar to the one exhibited in Fig.12b is observed. Already in frame b) impurities in the paint can be seen. These move slowly (as compared with the speed of the water) downwards and the give rise to a pattern in the wavyness which can be interpreted as "criss-cross". This is perhaps best seen in the frames d)-g). Already in frame f) the first traces of stream-wise striations can be noticed. These become more and more pronounced as time goes and in frame l) only traces of the vortices are found. It should be noted that beginning with frame g) local separation takes place at the equator leaving a very pronounced trace of the same type as shown in Figs. 14 and 15.

#6. Local separation.

The observation made in the preceding experiments on the traces left in the coat where local separation takes place was followed up by experiments with a flat plate in which evenly distributed disturbances were made in its surface. Fig.17 shows how these disturbances are distributed

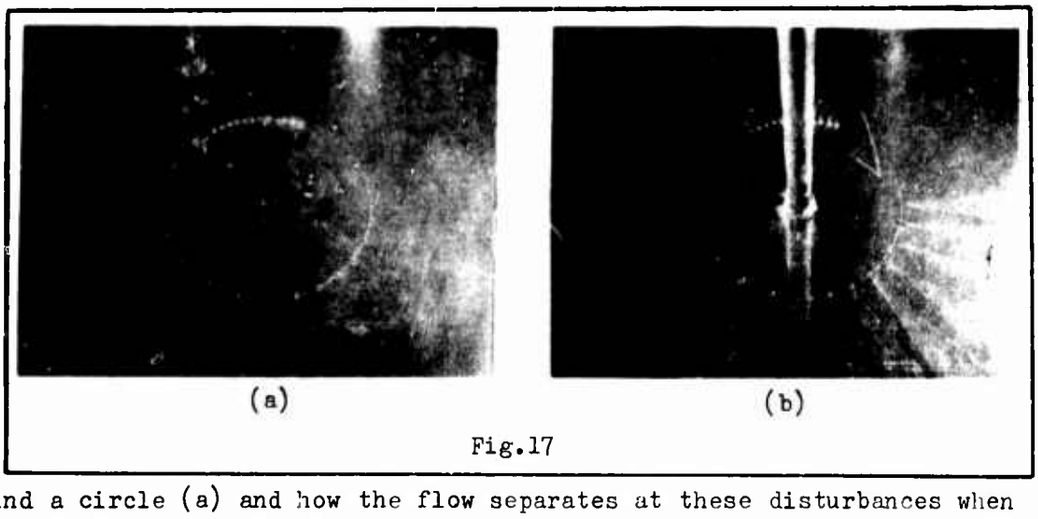

Fig.17

around a circle (a) and how the flow separates at these disturbances when the plate is exposed to the water jet (b). In fig. 17b the jet hits the plate

at right angle and the plate is not coated. Fig.18a shows a picture of the plate during a test run with a coat of paint having been applied outside the circle where the disturbances are. Fig.18b shows the pattern left in the coat by the action of the water. The coat is clearly affected much more in the region where local separation takes place (in the wake of a disturbance) than elsewhere. These experiments are still in progress and will be reported on elsewhere. They are here only touched upon because they represent a nice demonstration of the possibility to obtain information by rather simple means.

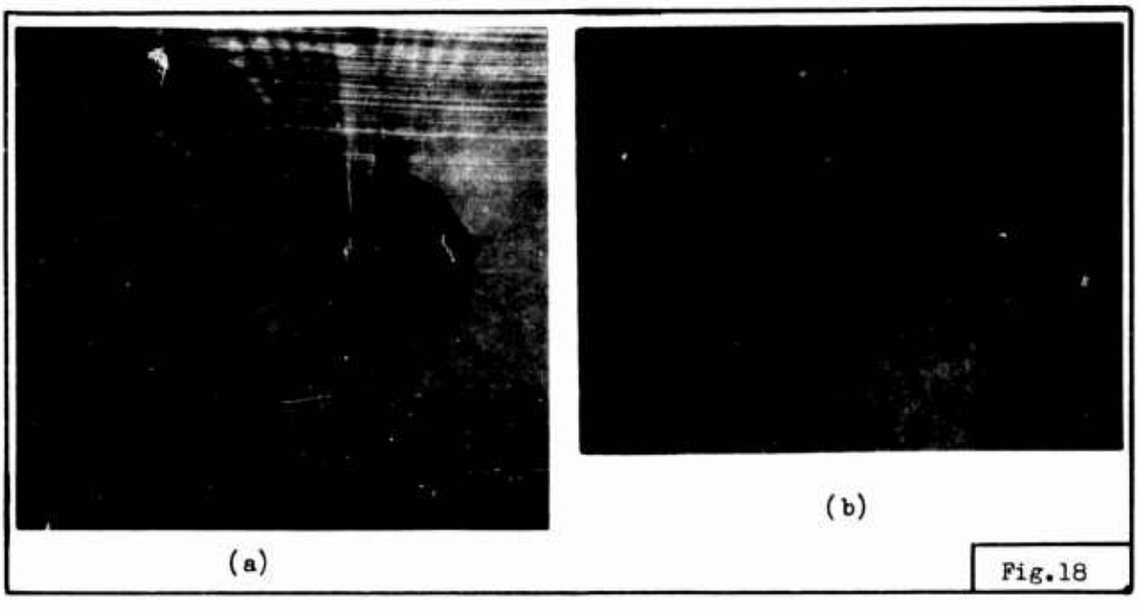

(a) (b)

Fig.18

#7. The water table experiment

The experiments with the water table were meant to give information on a two-dimensional flow situation which could be compared with the results obtained in the axis-symmetrical jet experiments. These experiments are still in progress and only two observations of qualitative nature will be mentioned here.

The flow conditions at the top of plate (A) (Fig.6) may be such that strong vortices (in the sense mentioned in the introduction) are formed in the flow before the water enters the upper edge of the plate. These are easily recognized because they cause a rippling of the light reflected from the shiny surface of the plate. Fig. 19 shows an example. These vortices are not stationary in the side-wise direction, and they show a very slow and apparently irregular (in time) change in their transverse location. This is due to the fact that these vortices are formed by irregularities in the flow

caused by the pump and the motion in the upper tank.

At the point where the vortex hits the lower plate (B),(Fig.6),

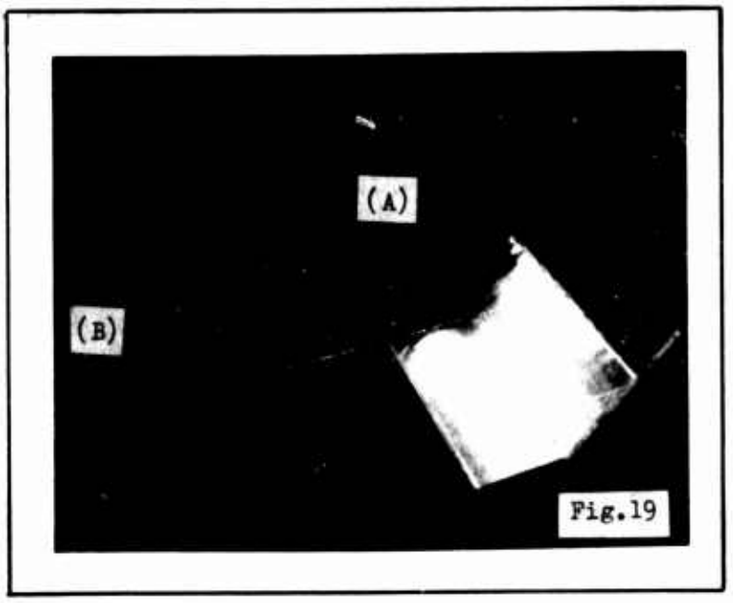

it gives rise to the formation of "bow-waves" as indicated in the sketch in Fig.20. It frequently also breaks down and causes an irregular motion of the water surface. This motion is very similar to the "turbulent spots" discussed by Emmons.[5]. A turbulent spot will however move downstreams

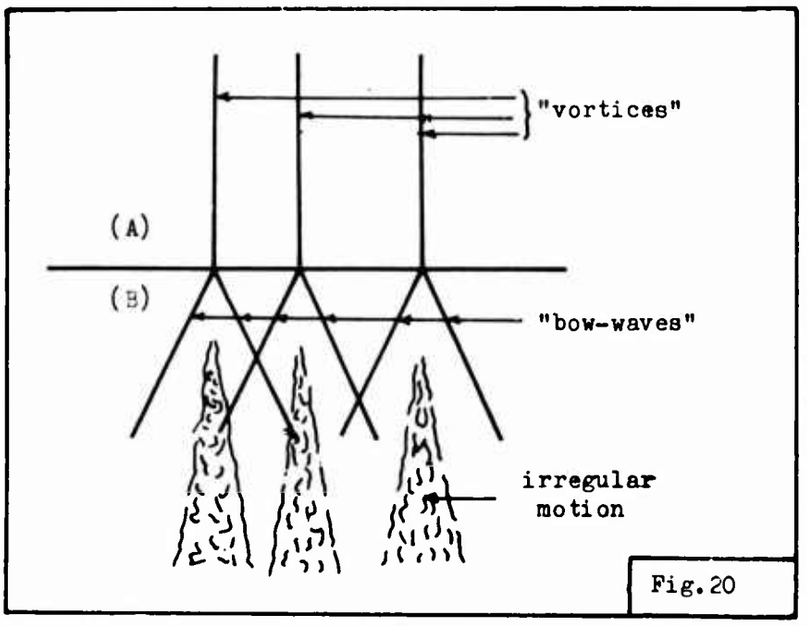

whereas the irregular motion in question here follows exactly the upstream vortex in its transverse location and stays stationary in its stream-wise direction. Fig.21 shows two different close-ups of the bow-waves.

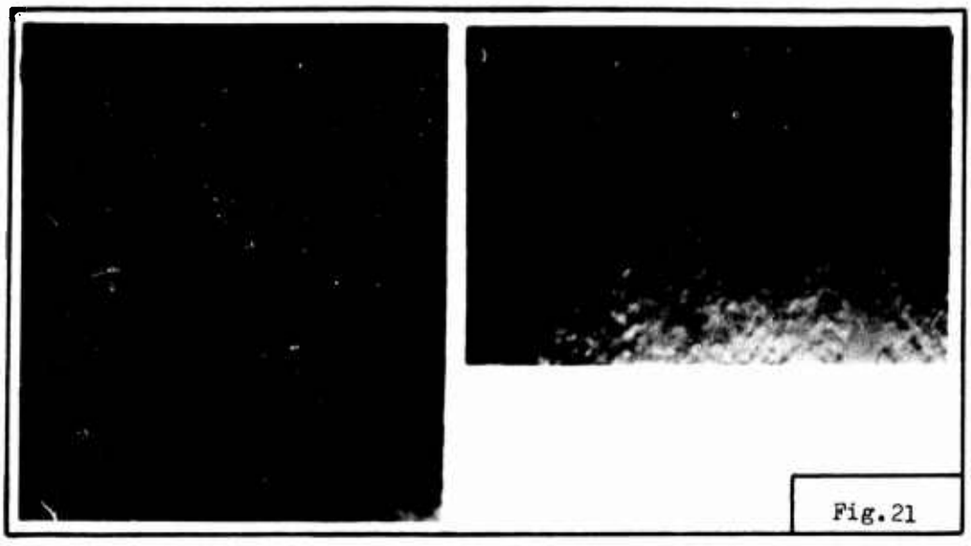

Fig.21

The phenomenon just described seems to have a direct bearing on the cross-hatching phenomenon shown in Fig.11. The present case may be thought of as a two-dimensional model of the axis-symmetric geometry in Fig.11 where stream-wise directed vortices will be formed on the upper part of the cone. Where these vortices hit the skirt a flow situation very similar to the one described in the water table experiment will occur. The hydraulic analogy for supersonic flow interprets the "bow-waves" as Mach-waves along wich disturbances will be propagated. These disturbances may in turn be responsible for the criss-cross pattern left in the surface. A more detailed study of this phenomenon is in preparation and here it is only mentioned to give substance to the need for a more detailed study of the vortex systems.

Another observation made in the water table experiment deserves mentioning. If the operating conditions of the table are arranged such that a very smooth and undisturbed flow is obtained, turbulent spots may be created by letting a drop of water drip down on plate (B). Under certain circumstances the disturbanes by the drop of water is unnecessary for the turbulent spots to occur. They are then probably created by disturbances in the flow. In either case they move downstreams with the flow, but a closer inspection shows that they always seem to be confined within a "bow-wave" on the upstream side. In a study of the ablation patterns A.L.Laganelli and D.E.Nestler [6] reported on a special type of pattern found on the surface of their Teflon

cone model. These are shown in Fig.22 which is reproduced from [6] and are described by the authors as follows: "-, the patterns appear to take the shape of a pair of dividers with a trailing vortex in the center. In most cases, the "handle" of the dividers appeared to initiate from an impact cavity resulting from debris in the tunnel flow field."

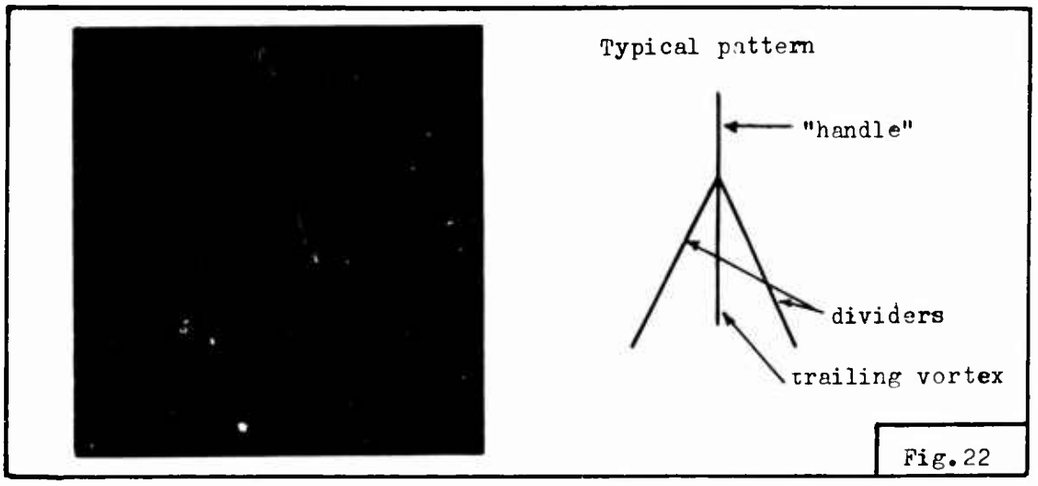

Fig.22

The two phenomenon drawn to attention here are different in the respect that the turbulent spot moves with the fluid whereas the pattern left on the Teflon cone is fixed in relation to the wall. Both cases seem however to have the break-down of a stream-wise directed vortex in common. If that is so the contention of the author [1] that such a break-down is part of the transition from laminar to turbulent flow may embrace even the turbulent spot. In the case described in Fig. 22 the vortex is induced by a particle hitting the surface. The vortex remains stable only over a short distance and breaks down giving rise to the dividers and the trailing "vortex". It is emphasized that these remarks are to be considered as speculations rather than conclusions, but whatever way on chooses to look at it the importance of the stream-wise directed vortex seems to stand out.

#8. The wave-lenght of the vortex systems.

The possilbe existence of stream-wise directed vortex systems in fluid flow under certain conditions is not only generally recognized but one is tempted to state that it has been experimentally proved. This experimental proof consists in most cases of stream-wise directed striations observed on the walls along which the fluid is flowing or in some kind of coat with which this wall is covered. Very little seems to be known about

the mechanical process responsible for the formation of these striations. The same holds true for the geometry (i.e. wave-length or transverse spacing) of these systems, for the origin of the vortex systems and several other questions connected with them. An attempt is here made to perform experiments with the water-jet to shed light on some of these questions.

As a starting point it was determined to fix the attention only on the striations which would occur in the coat of wet paint applied to the models when these were exposed to the water-jet. Any speculations or conclusions drawn from the direct observations to the flow field will be deferred until later. Three different models were used; one cone with a total cone-angle of 30°, one with 90° (both shown in Fig.23) and a flat plate (total "cone-angle" 180°). The paint used for the coat was an oil base enamel undercoat of the commercial type. The tests were performed with the axis of the cones coinciding with that of the jet thus leaving an axis-symmetric geome-

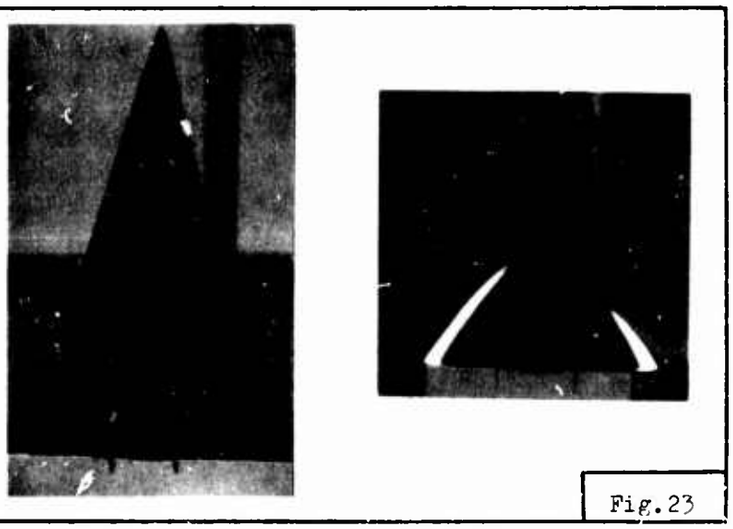

Fig.23

try. Three nozzles were used (see #2) to enable a variation in the thickness of the film of water flowing along the surface. The drying time allowed for the coat before the model was inserted into the jet was kept constant to secure equal test conditions. The running time for each test run was determined by inspection of the process as it developed. The run was terminated when the striations in the coat were clearly developed and the running time was recorded. Examples showing the type of striations observed in the coat are given in Fig.24. The striations can easily be counted and by dividing this num-

ber by the angle over which they appear a non-dimensional "wave-length" λ is obtained. (The angle in question is the angle in the cylindrical coordinatesystem whose axis coincides with the axis of symmetry.)

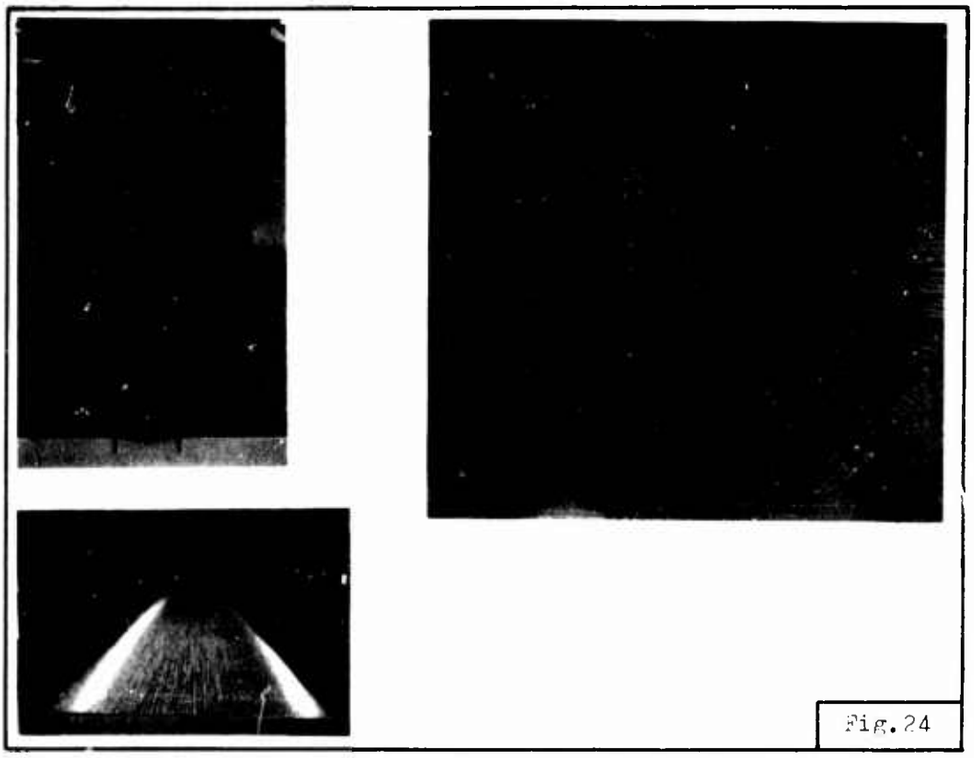

Fig.24

Because the tests were to be made with different speeds of the jet it was necessary to correlate the readings Δp of the manometer to the speed of the jet. This was done by taking discharge measurements which were timed. By dividing the discharge per unit time by the area of the nozzle opening the velocity was obtained. The correlation for the 3/8" and the 1/4" nozzles was the same whereas the correlation for the 1/8" nozzle deviated slightly as shown in Fig.25. This is accounted for by the slightly higher losses in the nozzle with the smaller opening. With the results of Fig.24 it is possible to correlate the results of the experiments with either $\sqrt{\Delta p}$ or the velocity v_0 of the jet.

The conditions under which the system operated during these tests are perhaps best characterized by the Reynolds' numbers of the jet and of the tube. The range of variation for Re_{tube} and Re_{jet} is given in Table I. It is realized that the flow in the jet is always turbulent whereas the flow in the pipe may be either turbulent or laminar according to the combination of jet speed and nozzle size.

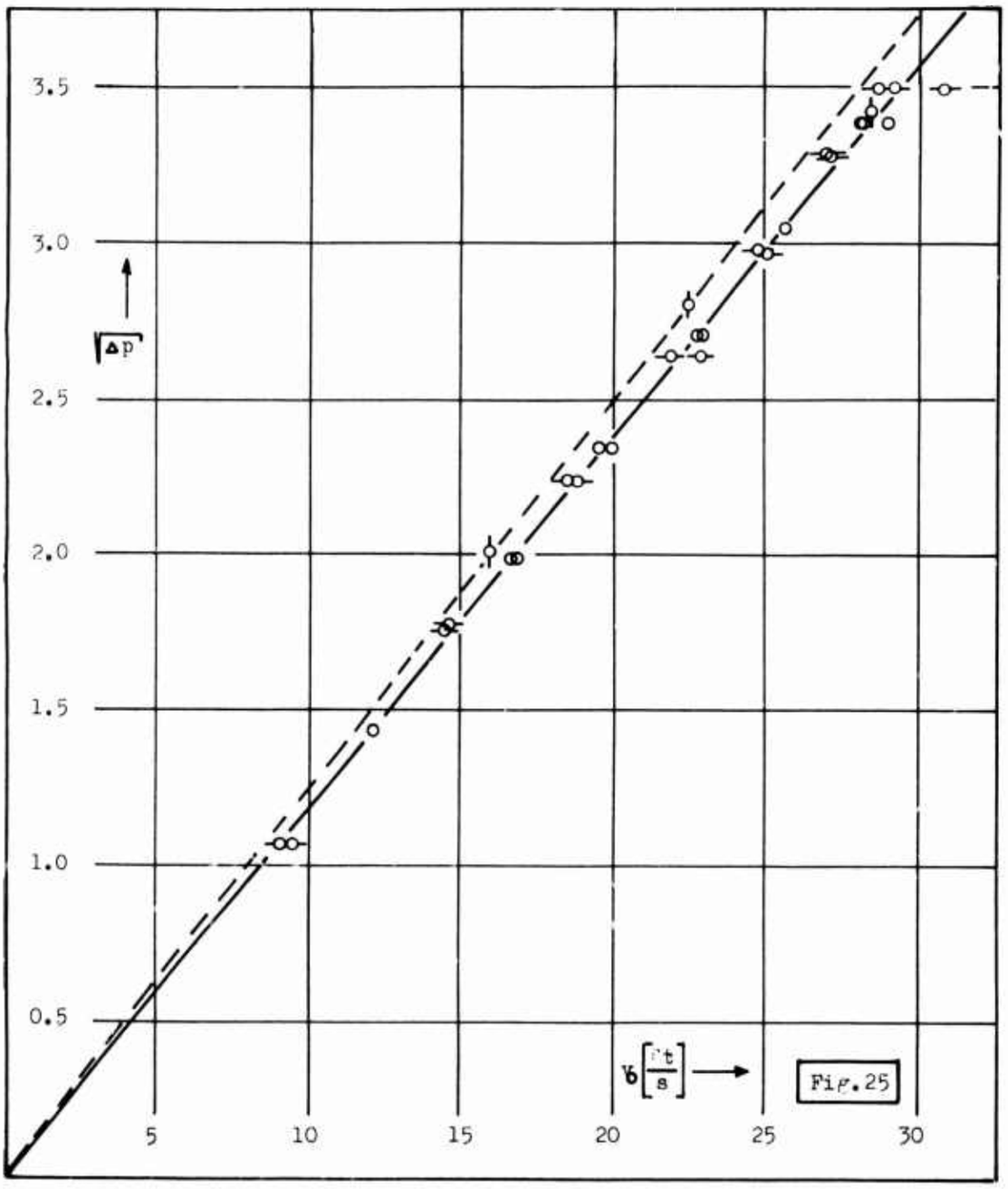

Table I	Re_{jet}			Re_{tube}		
v_{jet} =	10	20	30	10	20	30
1/8" Nozzle	9557	19113	28670	597	1195	1792
1/4" Nozzle	19113	38226	57339	2389	4778	7167
3/8" Nozzle	28670	57339	86009	5375	10751	16127

All three models were tested using all three nozzles whereby the speed of the jet was varied within the range mentioned. In this way a rather wide range of flow conditions were obtained. It turned out that a remarkable consistency exists in the results in the sence that if the number of striations per degree angle (λ) is plotted against $\sqrt{\Delta p}$ the results will be gathered on a straight line. Fig. 26, 27 and 28 show the results

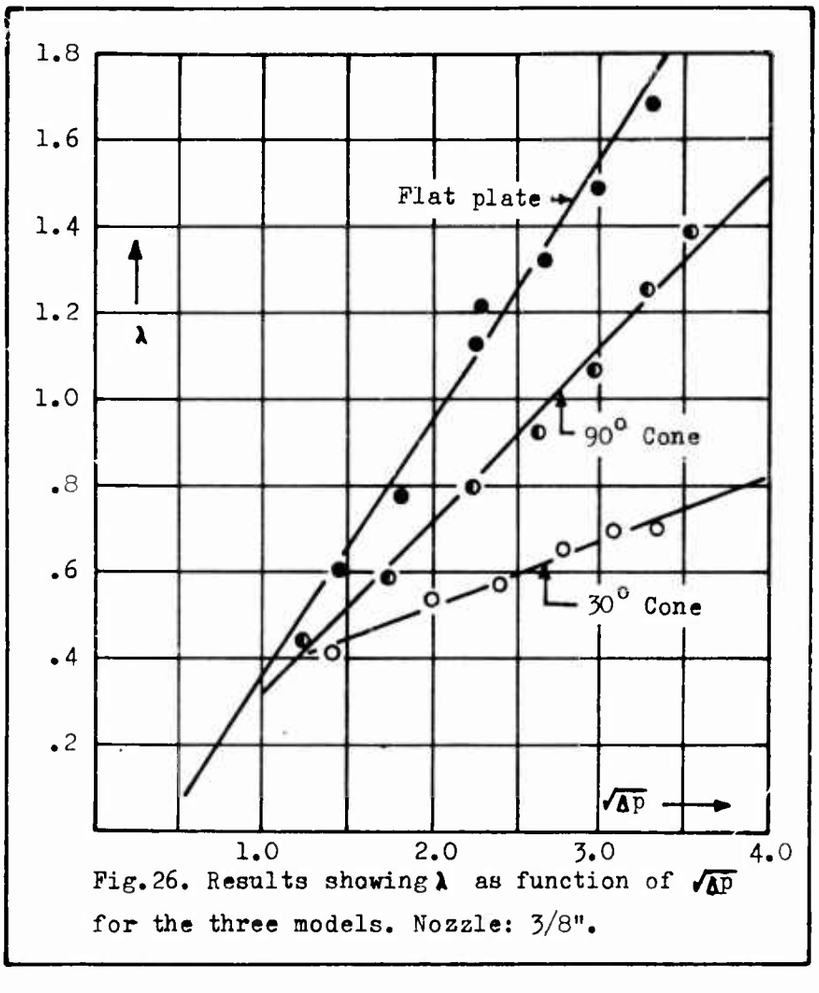

Fig.26. Results showing λ as function of $\sqrt{\Delta p}$ for the three models. Nozzle: 3/8".

for the three models, each Fig. giving the result for one nozzle only. The results mean that a linear relationship exists between the number of striations per degree angle and the velocity of the jet. The linearity in the experimental data is surprisingly good.

To bring out more clearly the relationships involved in the data the results are cross-plotted in Fig. 29, 30 and 31. These show the

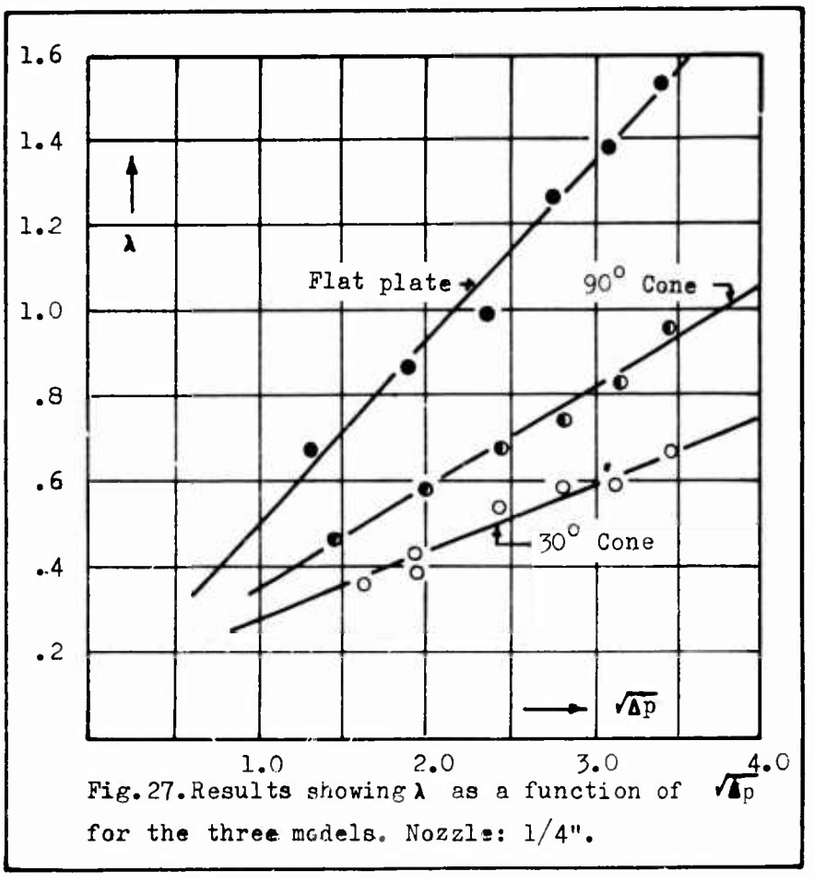

Fig.27. Results showing λ as a function of $\sqrt{\Delta p}$ for the three models. Nozzle: 1/4".

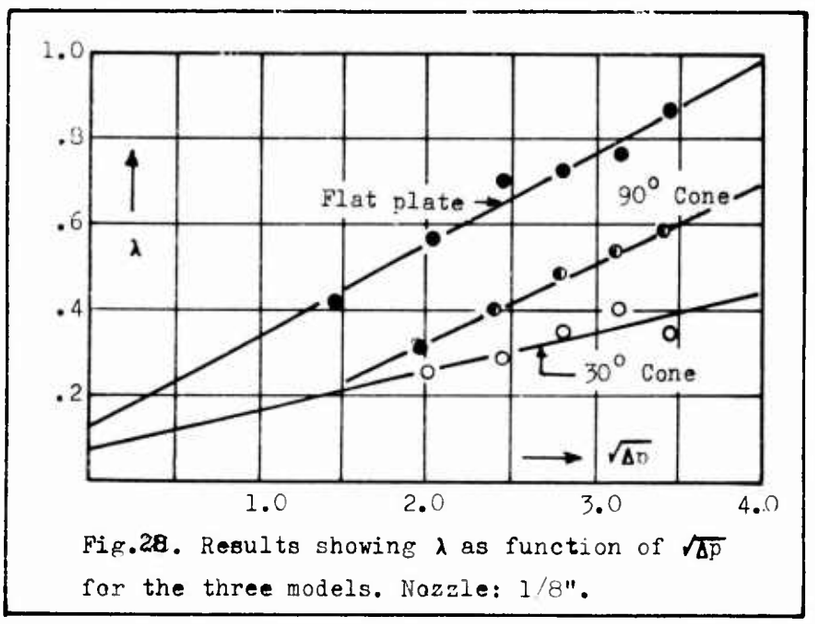

Fig.28. Results showing λ as function of $\sqrt{\Delta p}$ for the three models. Nozzle: 1/8".

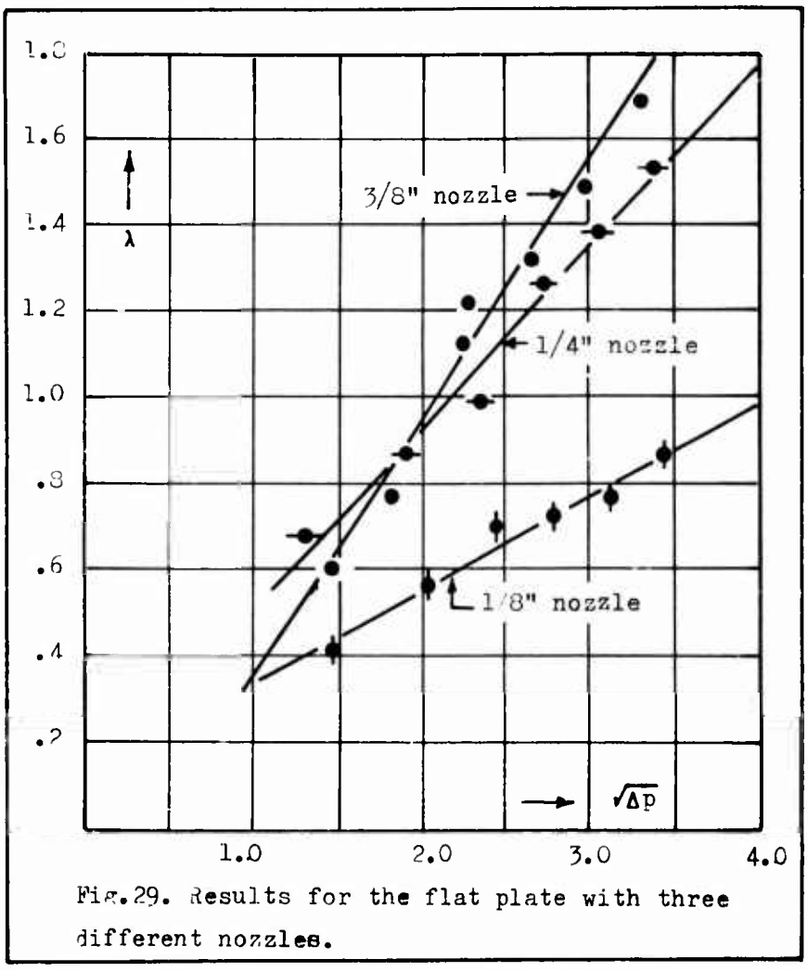

Fig.29. Results for the flat plate with three different nozzles.

results for each separate model in dependence of the size of the nozzle used. It should be noted that with the 1,8" nozzle it was very difficult to obtain clear striations on the 30° cone for low jet speeds. For that reason no observation appears in Fig. 31 for values of $\sqrt{\Delta p}$ less than 2.0 corresponding to a jet speed of 16 [ft/sec].

Two additional observations made during these experiments deserve to be mentioned. The experiment in #3 indicates the possibility that the number of striations may be dependant on the running time just as the number of heaps of sand was. This would mean that a tendency would be present for the striations to merge as the heaps of sand did. By keeping all conditions unchanged in two experiments with different running time it was observed that the number of striations was unchanged even though the running time

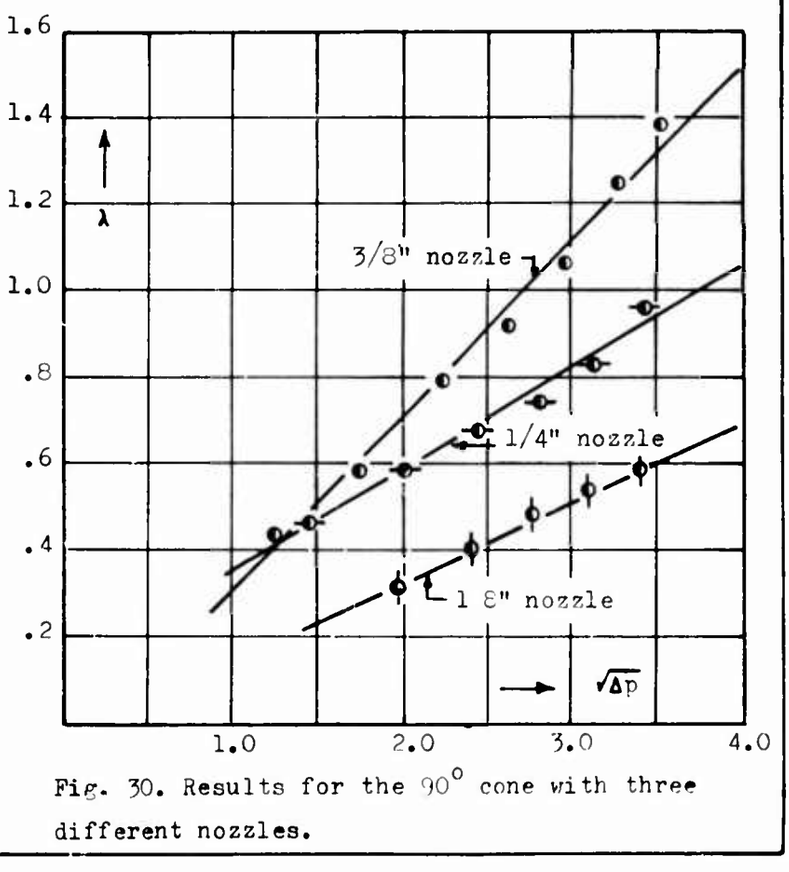

Fig. 30. Results for the 90° cone with three different nozzles.

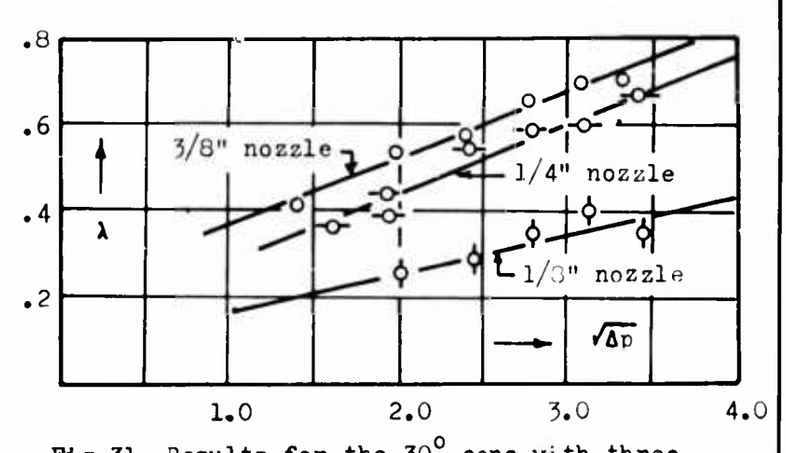

Fig. 31. Results for the 30° cone with three different nozzles.

was changed by a factor of 5. Thus: The striations do not seem to undergo a long-time change as far as their transverse spacing is concerned. (See further comments on this point in #12)

Because the coat used to exhibit the striations itself is a fluid the possibility exists that the number of striations is not only depending on the outside flow, but that some sort of interaction between the fluid and the coat may influence the number of striations. Even though an oil base paint was used as coating material to prevent a solution with the water, an interaction is still feasible. One factor that in such a case would be essential would be the viscosity of the coat. This possibility was investigated by repeating experiments under fixed conditions with the paint coat thinned to various degree. No viscosity measurements were made, but the paint was thinned so much that the time necessary for the striations to develop went down by a factor of 5. Within the accuracy of the measurements no change in the results could be detected. Thus: It seems reasonable to exclude the the influence of a possible interaction between the fluid and the coat on the transverse spacing of the striations.

(Remark: It should be noted that when the ablation process is studied, the thinning of the coat is crusial to the success of the experiments. This is explained in detail in a subsquent report on ablation.)

#9. Examination of the jet.

The results exhibited so far display a good degree of regularity but it is expected that they may reveal further information if they are correlated through the proper parameters. It seems natural to use the Reynolds' number Re_{jet} as such a correlating parameter but attempts show that the data do not correlate straight forward with this parameter. It was therefore necessary to examine the jet both theoretically and experimentally. The theory is confined to the flow on the flat plate outside the immediate stagnation region and inside the region bounded by the hydraulic jump. The theory is based on the assumption that the flow is turbulent and that Spalding's formulation of the law of the wall is applicable. An exposition of the theory is given in Appendix I.

First the jets were traversed with a static probe as sketched in Fig. 32. It was verified that the readings from the probe for any position within the jet did not vary by more than 2/10 " of water. It could therefore be concludeed that an even velocity distribution was present in the jets.

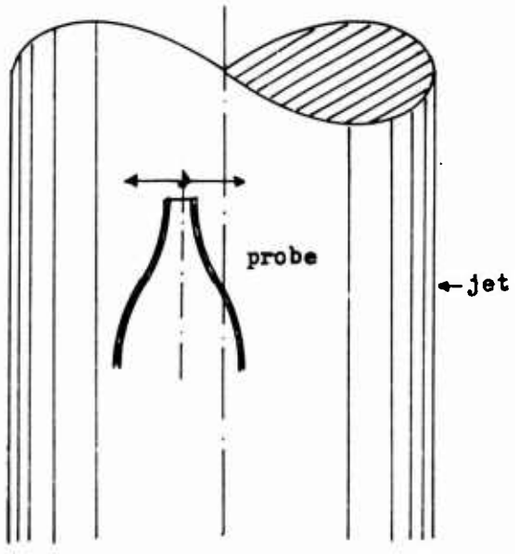

Fig. 32. Sketch of traversing probe in water jet.

The readings p_{st} from the probe correlated extremely well with the readings of Δp in the nozzle. For the 1/8" nozzle the results are given in Fig. 33. It is noticed that p_{st} is measured in inches of water whereas Δp is measured in inches of mercury. The straight line through the measured points is determined by means of a best fit according to Gauss' least mean square method. The slope is determined at 13.591 (sp.w. of mercury 13.58) and the vertical axis is cut at p_{st}=3.67". This corresponds to the free fall of the jet before it hits the probe and it shows that the influence of gravity on the jet between leaving the nozzle and hitting the plate must be corrected for if proper correlations are to be obtained.

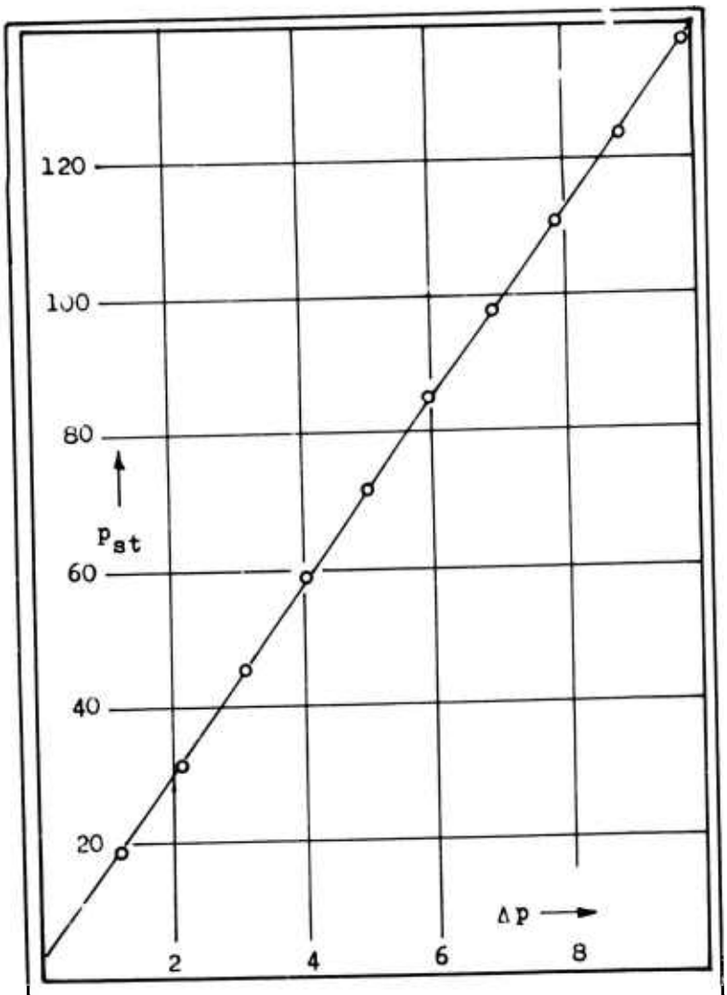

Fig.33. Correlation between p_{st} measured in inches of water and Δp measured in inches of mercury.

The needed correction for the influence of gravity will here be introduced based on elementary considerations of continuity and mechanics of freely falling bodies. Referring to Fig.34 the velocity v of the jet after a drop h will be

$$v = v_o + \sqrt{2gh} \tag{9.1}$$

The continuity of the jet gives

$$vd^2 = v_o d_o^2 \tag{9.2}$$

From these two relations the following corrected parameters are deduced:

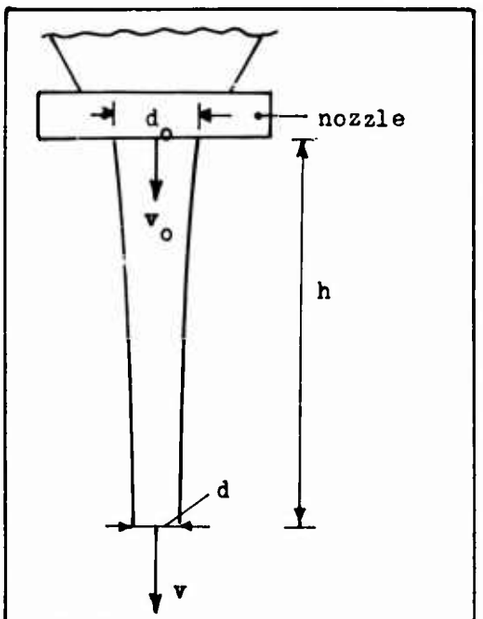

Fig. 34. Sketch of jet under the influence of gravity.

Corrected Reynolds' number

$$Re_{jet}^{corr} = Re_{jet}\left[1 + \frac{\sqrt{2gh}}{v_o}\right]^{+\frac{1}{2}} \qquad (9.3)$$

Corrected length

$$d = d_o\left[1 + \frac{\sqrt{2gh}}{v_o}\right]^{-\frac{1}{4}} \qquad (9.4)$$

The use of these corrections will be shown later.

As a next step the distribution of the static pressure p_s on the plate was measured. This distribution will be some kind of a "hat-curve" which in the stagnation region may be approximated by a parabola. The measurements were made for all three nozzles at fixed values of Δp and the parabolas were determined through a best fit using Gauss' method of least mean squares. The results are shown in Figs. 35, 36 and 37. It is noticed that the parabolas determine an inner region over which the pressure is distributed which is independant of Re_{jet} to within the accuracy of the measurements. The radiae r_i of these regions are given in Table II and it it noticed that the ratio r_i/r_o seems to be constant for all measurements.

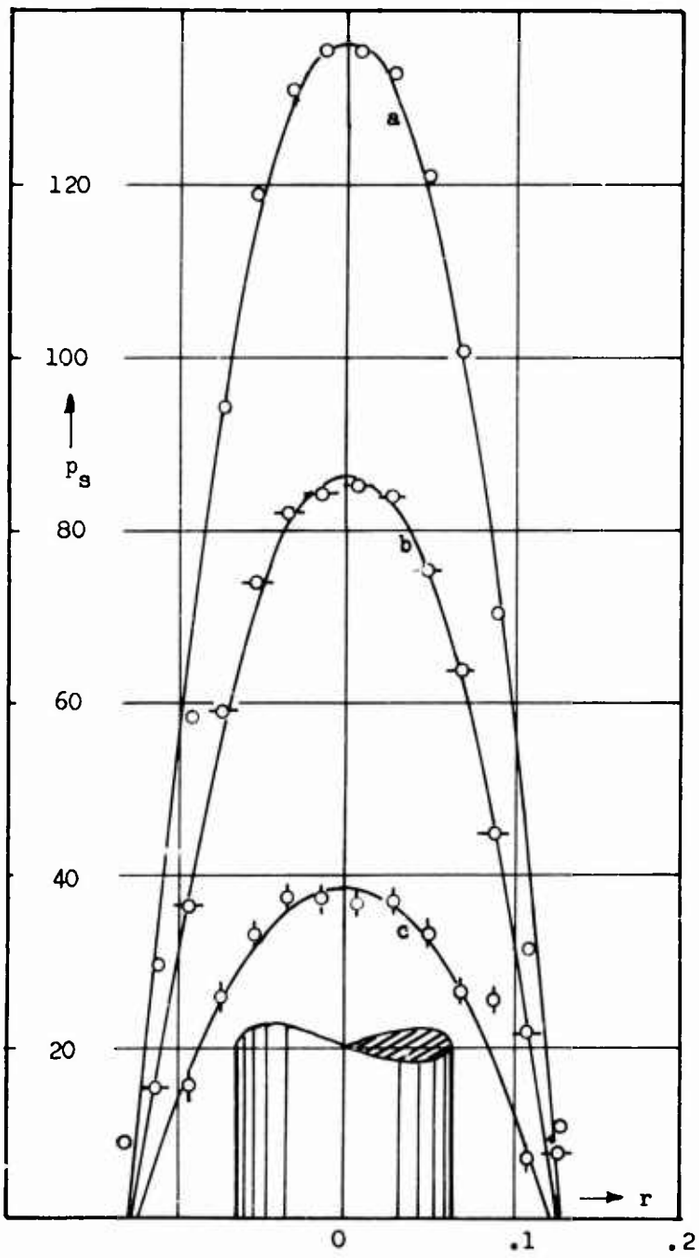

Fig.35. Pressure distribution on the plate with the 1/8" nozzle. r measured in inches, p_s in inches of water.
Curve a: Re_{jet} = 23 930
Curve b: Re_{jet} = 18 650
Curve c: Re_{jet} = 11 090

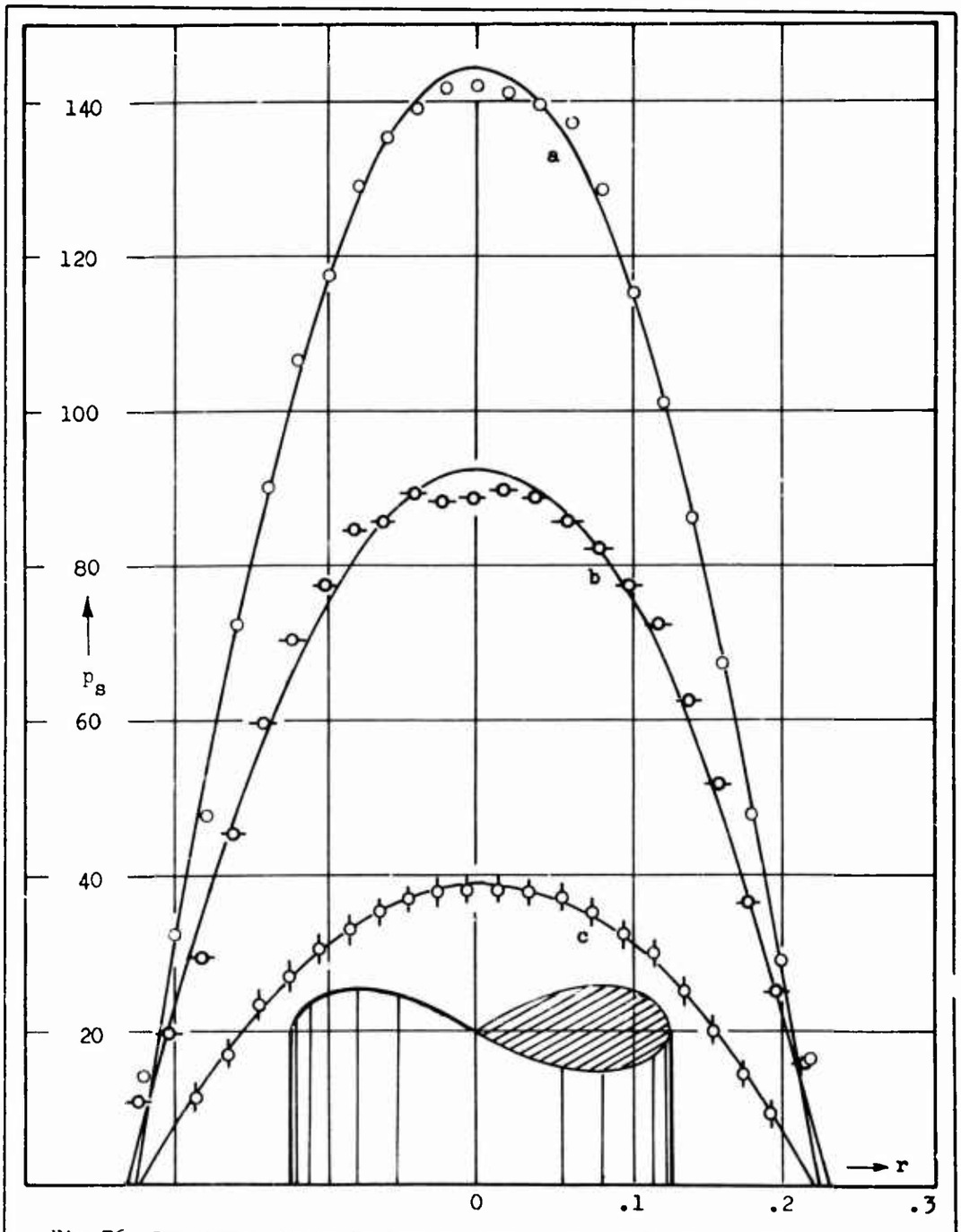

Fig.36. Pressure distribution on the plate with the 1/4" nozzle.
r measured in inches, p_s measured in inches of water.
Curve a: $Re_{jet} = 50\ 480$
Curve b: $Re_{jet} = 39\ 340$
Curve c: $Re_{jet} = 23\ 390$

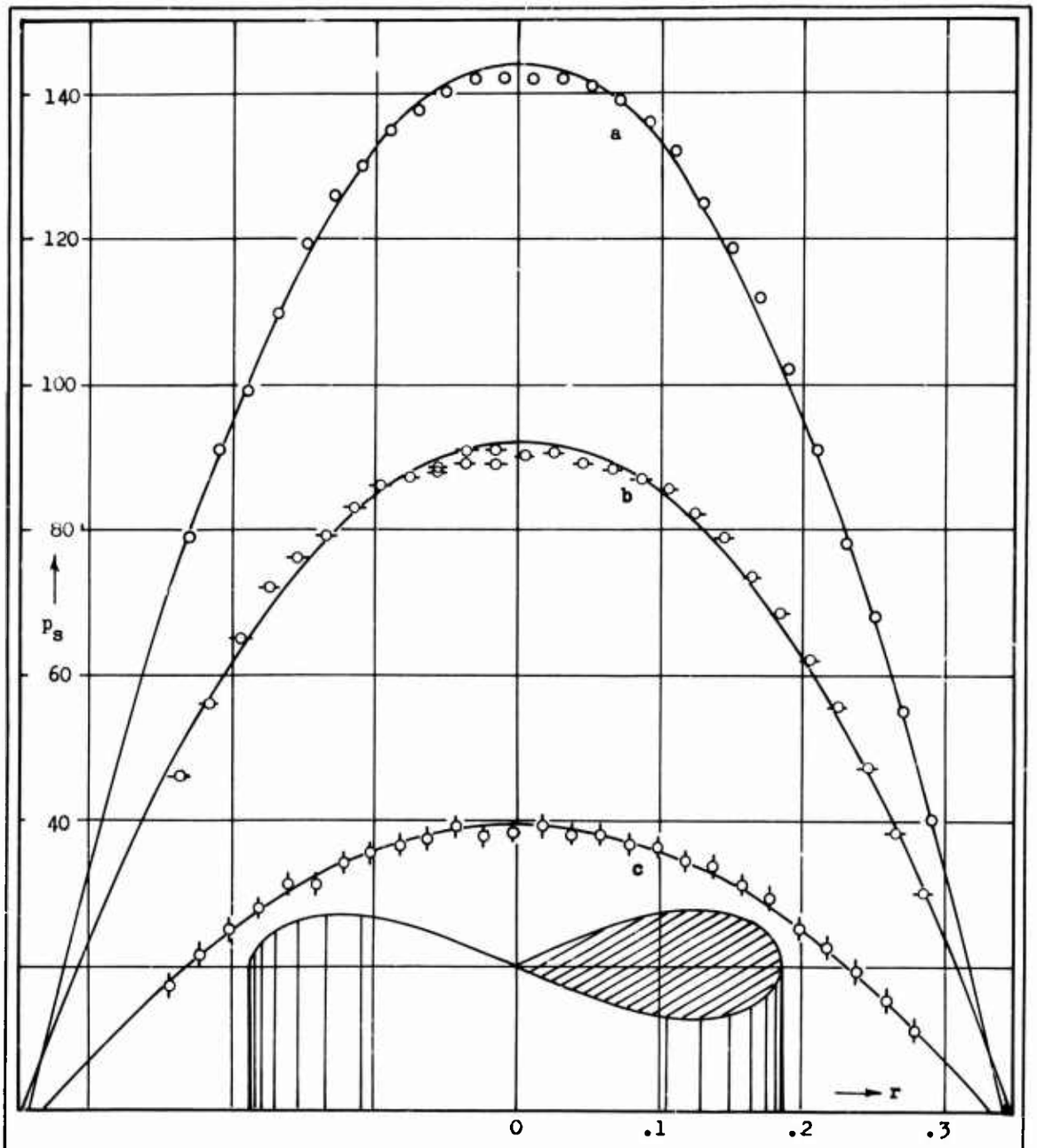

Fig.37. Pressure distribution on the plate with the 3/8" nozzle. r measured in inches, p_s in inches of water.

Curve a: $Re_{jet} = 75\ 340$

Curve b: $Re_{jet} = 58\ 720$

Curve c: $Re_{jet} = 34\ 910$

Table II	r_i	r_i/r_o
1/8" noz.	.118	1.89
1/4" noz.	.225	1.80
3/8" noz.	.340	1.81

It should be noted that r_o here denotes the nominal radius of the nozzle opening and that no correction of length according to (9.4) has been applied.

The preceding tests were mainly performed to make sure that the experimental set-up performed satisfactory and to make sure that the measurements were reliable. From there on it was natural to turn to a possible verification of the theory outlined in Appendix I. Equation (2.9) in Appendix I represents the continuity equation and is presumably valid for all jets under consideration irrespective of the value of Re_{jet}. The fact that the flow on the plate gives rise to a hydraulic jump furnishes a possibility for a very simple verification. The general validity of (2.9) would namely require $L(\zeta)$ to have a unique value at the position where the hydraulic jump occurs. Thus the quantity $Re_{jet}/4\zeta$ should be uniquely fixed at this position.

The position $r = R$ of the hydraulic jump and the corresponding nozzle pressure Δp was measured. From the latter reading the nominal exit velocity v_o from the nozzle as well as Re_{jet} can be computed in the following way (using the nominal diameter d_o of the nozzle and the results in Fig.25.)

$$\text{1/8" nozzle:} \quad v_o = \sqrt{\Delta p}/.1251 , \quad Re_{jet} = 7639.15\sqrt{\Delta p}$$
$$\text{1/4" nozzle:} \quad v_o = \sqrt{\Delta p}/.1186 , \quad Re_{jet} = 16115.64\sqrt{\Delta p}$$
$$\text{3/8" nozzle:} \quad v_o = \sqrt{\Delta p}/.1192 , \quad Re_{jet} = 24051.78\sqrt{\Delta p}$$

where Δp is to be introduced in inches of mercury. The non-dimensional radial distance ζ is formed with the nominal radius r_o of the nozzle according to (2.8) in Appendix I. Using these relations it turns out that the results of the measurements do not yield the desired relation. If however Re_{jet} is replaced by Re_{jet}^{corr} according to (9.3) and ζ is formed with d/2 from (9.4) instead of r_o the result will be as shown in Tables III, IV and V. In these tables the measured values as well as the computed relations are given. The corrections introduced accounted for a drop h = 12".

Table III (1/8" nozzle)

R	Δp	Re_{jet}^{corr}	Re_{jet}^{corr}/ζ
3.25	11.350	$2.93\ 10^4$	642.4
3.00	10.580	$2.84\ 10^4$	677.4
2.75			
2.50	4.900	$2.04\ 10^4$	614.4
2.25	3.360	$1.74\ 10^4$	602.0
2.00	2.205	$1.47\ 10^4$	594.1
1.75	1.340	$1.21\ 10^4$	589.7
1.50	1.045	$1.10\ 10^4$	645.0
1.25	.565	$.88\ 10^4$	670.5
1.00	.373	$.76\ 10^4$	770.8*

Mean value of Re_{jet}^{corr}/ζ
(excluded values marked *)
629.4 ± 34.2

Table IV (3/8" nozzle)

R	Δp	Re_{jet}^{corr}	Re_{jet}^{corr}/ζ
10.5	5.960	$6.93\ 10^4$	1459.3
10.0	5.575	$6.73\ 10^4$	1496.3
9.5	5.000	$6.43\ 10^4$	1515.4
9.0	4.325	$6.04\ 10^4$	1521.3
8.5	3.650	$5.63\ 10^4$	1521.0
8.0	2.975	$5.17\ 10^4$	1511.4
7.5	2.300	$4.66\ 10^4$	1487.0
7.0	1.915	$4.33\ 10^4$	1507.6
6.5	1.530	$3.96\ 10^4$	1521.7
6.0	1.146	$3.54\ 10^4$	1523.0
5.5	.855	$3.17\ 10^4$	1542.1
5.0	.566	$2.37\ 10^4$	1540.8
4.5	.277	$2.12\ 10^4$	1485.4

Mean value of Re_{jet}^{corr}/ζ

1510.2 ± 23.2

Table V (1/4" nozzle)

R	Δp	Re_{jet}^{corr}	Re_{jet}^{corr}/ζ
7.0	12.415	$6.40 \cdot 10^4$	1287.8**
6.5	8.560	$5.43\ 10^4$	1201.6*
6.0	5.960	$4.64\ 10^4$	1139.1
5.5	4.515	$4.12\ 10^4$	1126.8
5.0	3.165	$3.55\ 10^4$	1100.1
4.5	2.395	$3.17\ 10^4$	1118.7
4.0	1.720	$2.78\ 10^4$	1139.7
3.5	.951	$2.21\ 10^4$	1108.9
3.0	.565	$1.82\ 10^4$	1143.6
2.5	.180	$1.23\ 10^4$	1108.6

Mean value of Re_{jet}^{corr}/ζ
(excluded values marked*)

1123.2 ± 16.6

Even though the measurement of the location of the hydraulic jump is difficult especially at high and low values of the jet velocity, the results show a remarkably good verification of the theoretical prediction, i.e. for each nozzle separately. Comparing the results from the different nozzles however a remarkable difference between them is brought to light. This requires an explanation. The quantity Re_{jet}^{corr}/ζ used for the verification is defined as follows

$$Re_{jet}^{corr}/\zeta = \frac{vd}{\nu} \cdot \frac{d}{2r} \qquad (9.5)$$

where d is given in (9.4) and v in (9.1). Now v is determined by means of the nominal velocity v_o which is directly determined from the discharge measurements. (Fig.25.) The velocity v is therefore a legitimate velocity with which the flow on the plate can be characterized. The distance d is however arbitrarily chosen as a length with which the Reynolds' number is formed. This same length will according to the deduction in Appendix I of (2.9) enter the theory as the length with which the non-dimensional radial distance is being formed. In (9.5) it is seen that this lenth d enters the expression raised to the second power. It means that experiments performed with different nozzles can only be interrelated if the proper length is chosen to form the Reynolds' number, and the values of the parameter in (9.5) obtained from the hydraulic jump measurements and exhibited in Tables III,IV and V indicate that the nominal diameter of the nozzle d_o is not the proper length.

At this stage no attempt will be made to determine what the proper length should be because the following line of reasoning will provide a basis for the necessary re-correlation of the striation count data. Let d_3, d_2 and d_1 represent the proper lengths for the 3/8", the 1/4" and the 1/8" nozzles respectively. If now experimental data obtained with the three different nozzles and originally correlated through Re_{jet}^{corr} are to be compared, the Reynolds' numbers would for each nozzle have to be multiplied by the factors d_3/d_o, d_2/d_o and d_1/d_o respectively. However a comparison is still possible even if the threee lengths are not known but their ratios are known. In that case the comparison can be made if one arbitrarily chooses Re_{jet}^{corr} for the 3/8" nozzle as the correlating parameter and multiplies the corresponding parameter for the two other nozzles with a constant correction factor. In the case of the hydraulic jump experiment the results from the tables show the following situation. The mean value of Re_{jet}^{corr}/ζ varies very much from one nozzle to another. If however the length used to form the Reynolds' number as well as the non-dimensional radial distance with had been $1.16d_o$ instead

of d_o the mean value of the parameter for the 1/4" nozzle would have been 1510.2 as for the 3/8" nozzle. For the 1/8" nozzle the same would be the case if the length $1.549d_o$ had been used.

As a conclusion the following statement can be made: The Re_{jet}^{corr} parameter seems to be well suited as a correlation parameter for each nozzle separately. When results from different nozzles are to be compared the parameter will have to be adjusted by constant factors c_1, c_2 and c_3 which from the hydraulic jump measurements have been determined as follows:

$$\begin{aligned} &1/8\text{"nozzle: } c_1 = 1.549 \\ &1/4\text{"nozzle: } c_2 = 1.160 \\ &3/8\text{"nozzle: } c_3 = 1.000 \end{aligned} \qquad (9.6)$$

It is understood that one in this way only gets a relative comparison between the results, with the results from the 3/8" nozzle having arbitrarily been kept unchanged. It is however stressed that the numerical values in (9.6) are not to be considered satisfactorily determined. This point will be commented upon later.

#10. Re-correlation of data.

The results of the preceding section are now utilized for the purpose of exhibiting, if possible, a more general correlation of the striation count data of Figs. 29, 30 and 31. Through the relations given in #9 it is easy to convert the measured values of Δp into Re_{jet}^{corr} and with the factors of (9.6) the results for the flat plate from Fig. 29 are reproduced in Fig. 38. It is seen that the data now seem to have much more regularity in them and that they tend to determine a straight line valid for all data obtained on the flat plate. A closer examination shows however that the data apparently still have systematic deviations in them which may be due to an inadequate determination of the factors in (9.6). Instead of looking for other methods of determining the factors it is possible to switch the approach to the problem in the following way.

If it is stipulated as a fact that the data from different nozzles will correlate through the appropriate Reynolds' numbers if these are adjusted through constant factors for each nozzle as indicated in (9.6), then the actual values of these factors are already hidden in the data themselves and they can be brought out by a method of best fit. How this can be

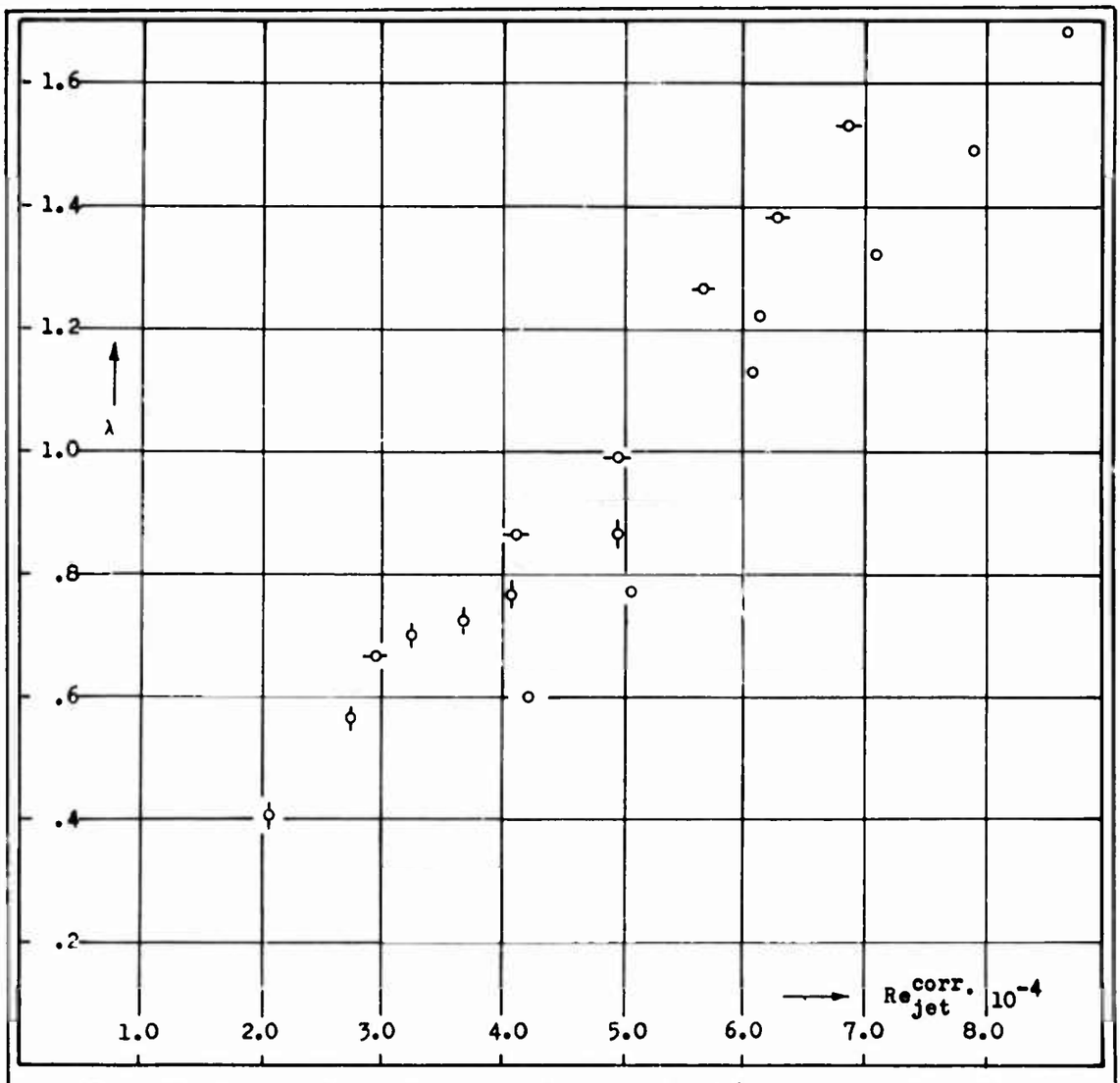

Fig. 38. Number of striations per degree angle (λ) correlated with the Reynolds' numbers adjusted with the factors from (9.6).
o : 3/8" noz. , -o- : 1/4" noz. , ϕ : 1/8" noz.

done is outlined in Appendix II. It is noticed that x_i and y_i represent the measured values of Re_{jet}^{corr} and λ respectively. The result of this procedure as far as correlation of data is concerned can be seen from Fig. 39. The fac-

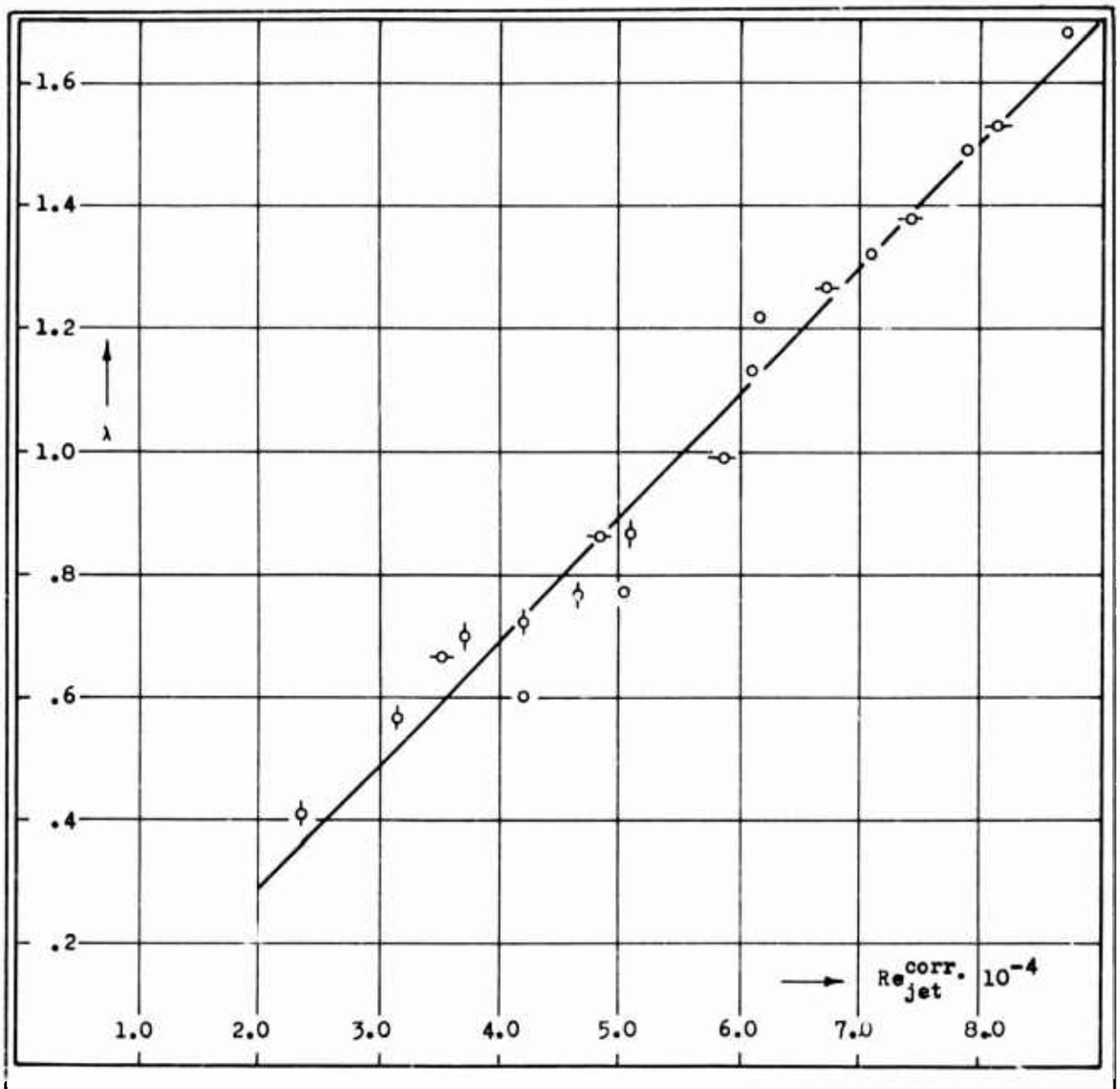

Fig.39. Re-correlated data from the striation count on the flat plate with the factors determined by a "best fit" procedure. (Corresponds to Fig.29)
o : 3/8" noz. , -o- : 1/4" noz. , ϕ : 1/8" noz.

tors c_2 and c_1 obtained from this procedure are given as

$$c_3 = 1.000 \quad , \quad c_2 = 1.374 \quad , \quad c_1 = 1.778 \qquad (10.1)$$

It is reassuring to see that the factors determined this way are very close to the factors determined from the hydraulic jump experiment. Further comments

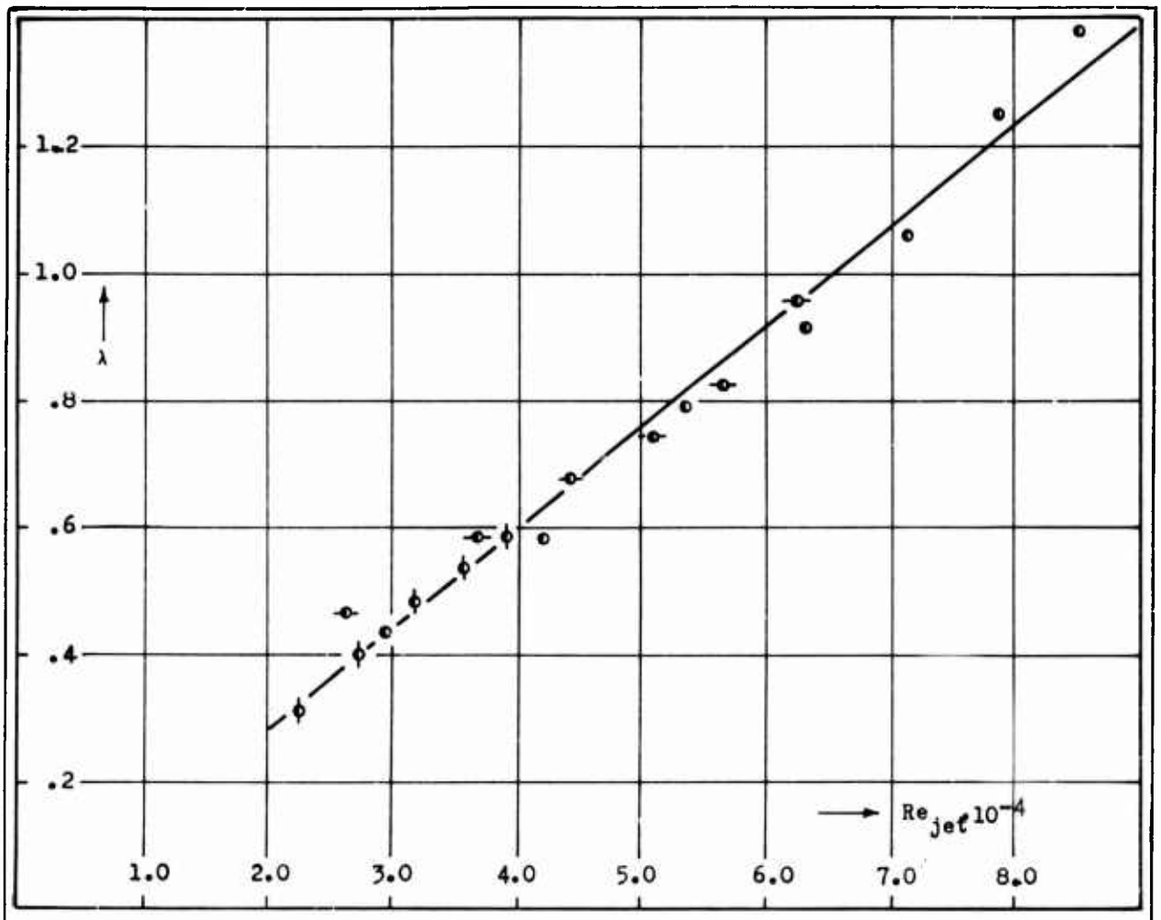

Fig.40. Re-correlated data from the striation count on the 90° cone; obtained from the same procedure as that used for the flat plate. (See Fig. 30.)
o : 3/8" noz. , -o- : 1/4" noz. , ϕ ; 1/8" noz.

on this point is deferred until later.

One reason why the method of correlation shown here was adopted was that it can be used without modification also for the results obtained on the cones. The only difference is that for both cones the drop from the nozzle to the tip of the cone was negligible and thus Re_{jet} should be expected to give an adequate information on the flow conditions at the cone tip. It is furthermore to be expected that also in this case factors will have to be introduced to enable a comparison between results obtained with

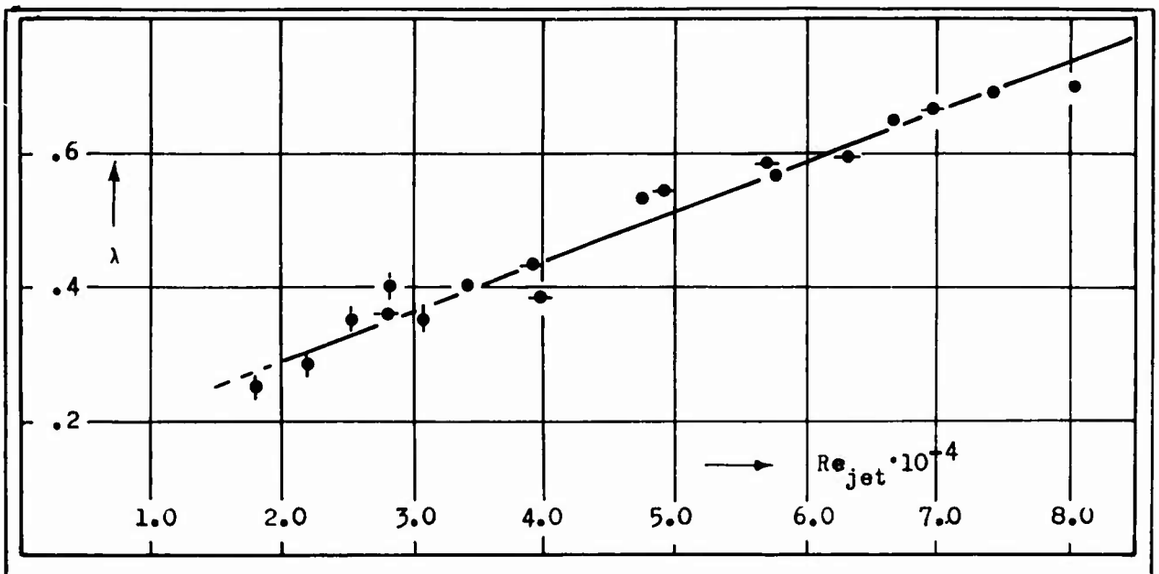

Fig. 41. Re-correlated data from the striation count on the 30° cone; obtained from the same procedure as that used for the flat plate. (See Fig. 31)
o : 3/8" noz. , -o- : 1/4" noz. , ϕ : 1/8" noz.

different nozzles. The magnitude of these factors may however be expected to decrease with the cone-angle. The result of this procedure is shown in Figs. 40 and 41 for the 90° and the 30° cones respectively. The values of the adjustment factors which give the the excellent correlation were computed as:

$$30^\circ \text{ cone: } c_3 = 1.000 \;,\; c_2 = 1.262 \;,\; c_1 = 1.184 \qquad (10.2)$$
$$90^\circ \text{ cone: } c_3 = 1.000 \;,\; c_2 = 1.128 \;,\; c_1 = 1.504$$

In spite of the astonishingly good correlations obtained and exhibited in Figs. 39, 40 and 41 one can not be entirely happy with the fact that the adjustment factors obtained do not exhibit a similarly good regularity. It means that the method used to compute these factors ("best fit procedure) may have over-beautified the results. Even so the results are adequate for bringing out what is thought to be some fundamental facts regarding the striations and the stream-wise directed vortices which cause them. It is hoped that this will become clear from the subsequent remarks.

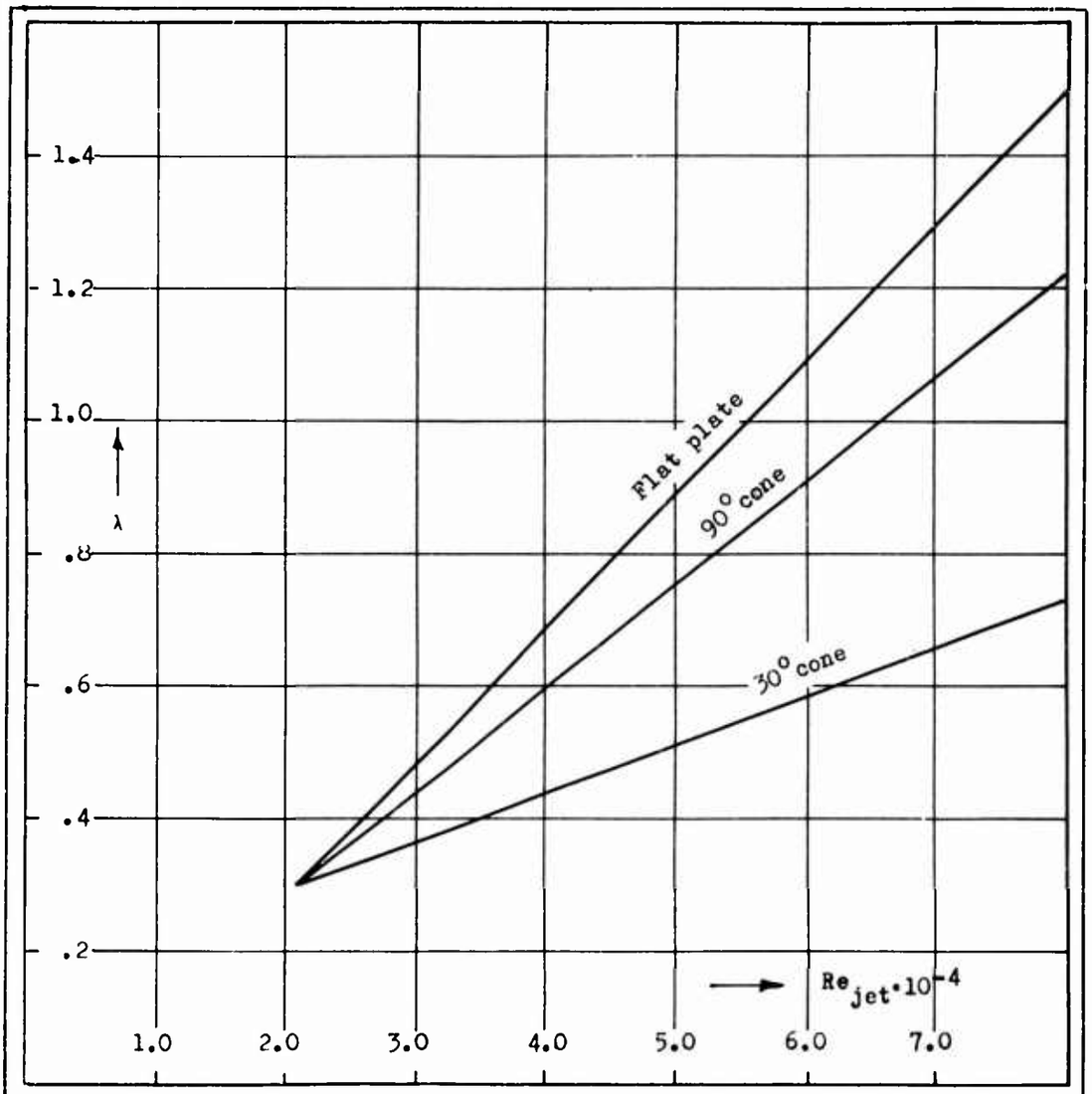

Fig.42. Plot of the results from Figs.39,40 and 41 showing the determined straight lines only.

Because the results in all cases have been correlated with unchanged values for the Reynolds' number for the 3/8" nozzle it is possible to compare the results for all models. This is done in Fig.42 where for the sake of simplicity only the determined straight lines are shown. These straight lines reveal some rather interesting features.

If one considers the physical reality behind the striations one will find it hard to envisage a case where only one, two or a few striations could be observed over the entire 360° of the models. This indicates that a "lower limit" will exist for λ. Fig. 42 reveals that the determined lines intersect (almost exactly) in one point. ($Re_{jet} = 2.1\ 10^4$, $\lambda = 0.3$) Even though the results in Fig.41 exhibit one point below the point of inersection, it is possible to interpret this intersection point as the lower limit. Without drawing too farfetched conlusions one may therefore say that the results so far have supported the contention that the stream-wise directed vortices (supposedly responsible for the striations) appear as a result of the basic (two-dimensional) flow becoming unstable. The vortices are characteristic of the stable three-dimensional flow that evelops. Because of the way in which the results are correlated, no criteria of stability can be given..

Fig.42 clearly brings out the fact that λ depends on the angle through which the jet is being deflected by the models. For the flat plate, the 90°cone and the 30°cone the angle of deflection is 90°, 45° and 15° respectively. The three lines in Fig.42 are:

Flat plate: $\lambda - 0.3 = 0.20274(Re_{jet}^{corr} \cdot 10^{-4} - 2.1)$

90°cone: $\lambda - 0.3 = 0.15742(Re_{jet} \cdot 10^{-4} - 2.1)$

30°cone: $\lambda - 0.3 = 0.07354(Re_{jet} \cdot 10^{-4} - 2.1)$

It is remarkable to notice that the ratios between the slopes of these lines are very close to the ratios between the sines of the deflection angle. This is perhaps best brought out by a hypothetical argument. Suppose that the slope of the line for any angle of deflection of the main jet were given by $0.2318 \cdot \sin\alpha$, where α is the angle. In the case of the models used here the slopes would be

for the flat plate:	0.2318	giving a deviation from the values above of	14.3%
for the 90°cone:	0.1639		4.1%
for the 30°cone:	0.0600		18.4%

This entirely within the degree of accuracy of the measurements.

The results of the experiments and the argument offered above seem to strongly indicate that the transverse wavelength of the striations

is proportional to the sine of the angle of deflection which in turn can be related to the curvature of the path of a fluid particle.

The correlation of data exhibited here may seem unusual because only a relative correlation is obtained. The reason for this is that the relation between all data could in this way be brought about, and the aim was to bring out general features of the problem. This could be done even if the correlation is only suited for the purpose of comparison. When these features have been exhibited it is tempting to attempt a correlation of the data from the flat plate which can render a more general insight in the problem.

#11. Final correlation of data

The correlation of the data attempted so far has exhibited some rather interesting features of the problem. However the results are only relative and the Reynolds' number of the jet does not seem to be the proper parameter to describe the phenomenon taking place on the surface of the models and in the water film. If the results are to be carried over to applications in air flow, a better correlation must be established using quantities which can be reinterpreted in air. The complete answer to this problem will not be attempted here but a very interesting correlation will be brought out.

The previos correlation brought out the fact that apparently a very special length is characteristic of the phenomenon under investigation and attempts to find this length were undertaken. The first and most obvious length that presented itself in this connection was the thickness of the water film. Direct measurements of this length were made, but the accuracy of the measurements was not adequate and further experiments will have to be made so that the results can be properly confronted with the proposed theory in Appendix I. Provisions for continued efforts in this direction have already been made.

It is at this stage natural to draw to attention the hypothesis that stream-wise directed vortices appear as a result of a curved flow becomming unstable. This idea was originally presented to the author by Dr. Max Scherberg and although no generally valid stability criterion has yet been presented, both the author's examination of available experimental evidence [1] and a recent thesis by R.T.Wood [7] strongly support this hypothesis. With this in mind it seems natural to use a Reynolds' number as correlating parameter which is built from the radius of curvature of the flow (R) (characteristic length) and the velocity (v) with which the fluid enters this

path (charateristic velocity).

The velocity v to be used here is different from the nominal velocity v_o and is deduced directly from the measurements described in Fig. 32 and Fig. 33. This gives directly the following relation between v and the measured value of Δp for each experiment on the flat plate

$$v^2 = 2p_{stat} = 2(13.6\Delta p + 4.5)/\rho \qquad (11.1)$$

where Δp is to be introduced in inches of Hg and where ρ must be introduced in the right dimension to give v in ft/sec. The additive term 4.5 is the correction for the free fall of the jet before impinging on the plate.

For the cone models no free fall of the jet was present and the nominal velocity v_o from #9 is used.

The radiae of curvature of the flow was determined from pictures taken of the flow as exhibited in Fig.43. The radius of curvature obtained this way is that of the water surface, the only one being directly measurable. Similar pictures were taken both of the flat plate and the 30° cone, for all nozzles and for a sequnce of different jet velocities. The measurements revealed that for each model and each nozzle the radius of curvature R remained constant to within the accuracy of the measuements, i.e. R is for a given setting independent of the jet velocity.

Fig.43. Measurement of R for the 90° cone. (3/8" nozzle)

The result of these measurements came out as follows:

Model	3/8" nozzle	1/4" nozzle	1/8" nozzle
Flat plate	R = .1105"	R = .0997"	R = .0505"
90° cone	R = .415"	R = .305"	R = .211"
30° cone	R = 1.988"	R = 1.800"	?

It is noticed that no measurement was obtained for the 30° cone with the smallest nozzle because the bluntness of the cone caused a dent to occur

in the surface of the small jet. Thus a measurement with any degree of accuracy was impossible.

The correlating Reynolds' number Re_R is defined as

$$Re_R = \frac{vR}{\nu} \qquad (11.2)$$

and Fig.44 shows the result of the striation count for the flat plate. The

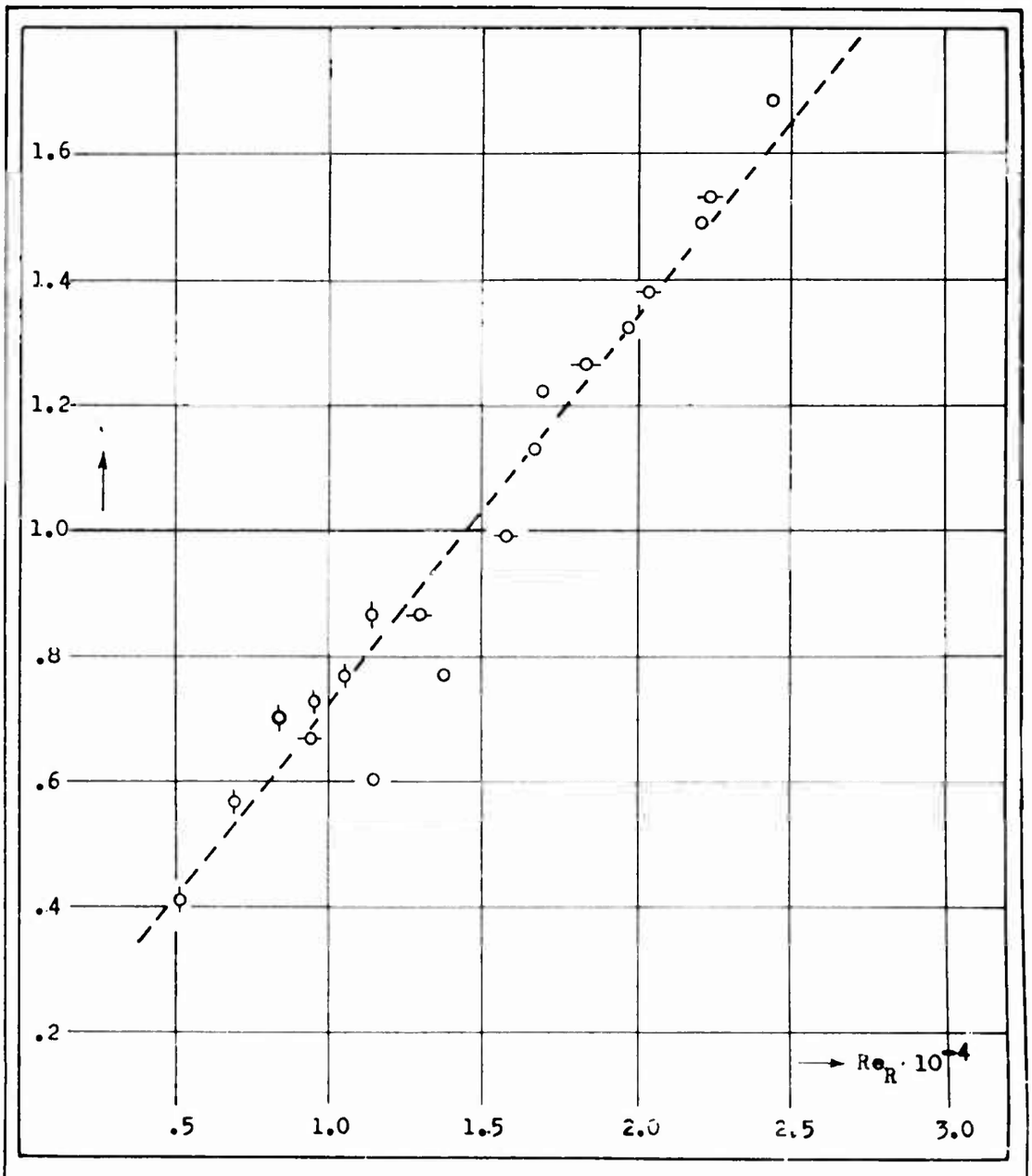

Fig.44. Results of the striation count for the flat plate showing λ as a function of Re_R

dotted straight line is plotted according to the best fit procedure. It is noticed that in spite of the seemingly good correlation obtained, the results from the 1/8" nozzle (marked ϕ) appear almost consistently above this line. This may be caused by an error in the measured value of R for this nozzle, which was very difficult to measure. As shown earlier the small jet did not give any results for the 30° cone.

Corresponding correlations of the results for the 90° and 30° cones are shown in Figs.46 and 45 respectively. Here the correlation is extremely good and the only tendancy to show systematic deviation from the dotted line is found in Fig.46 for the results from the 1/4" nozzle (marked -o-).

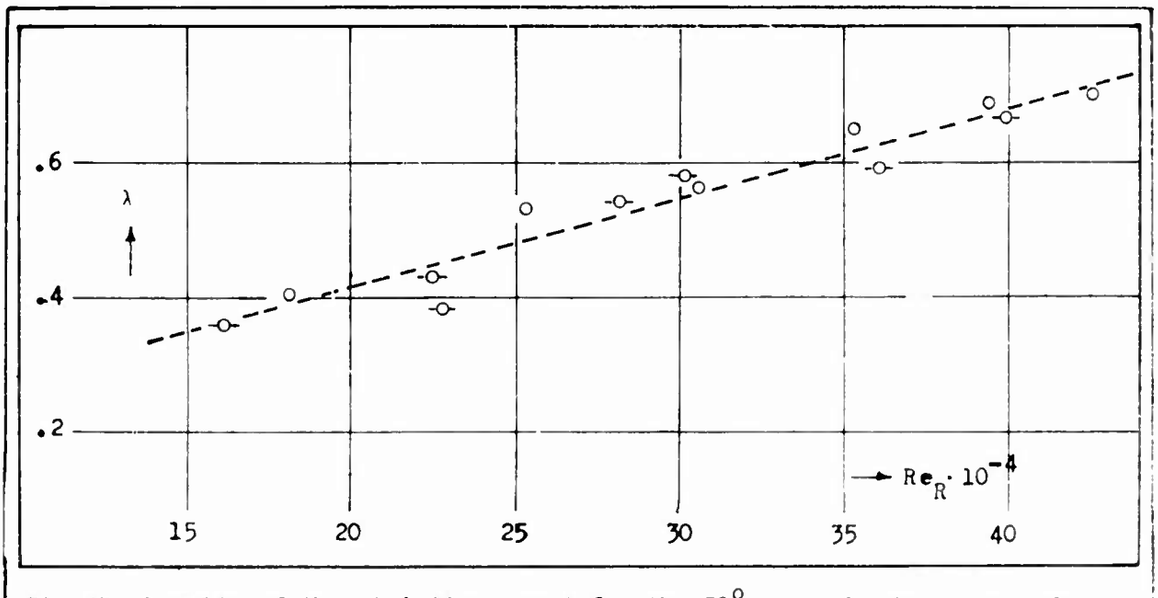

Fig.45. Results of the striation count for the 30° cone showing λ as a function of Re_R

One observes of course that now the absolute values of the correlating parameter vary very much from one model to another due to the fact that the radius of curvature R enters the chosen Reynolds' number.

In spite of the minor beauty-spots of the present correlation it is felt that the results exhibited strongly supports the contention that stream-wise vortex systems occur as a result of the curved flow becoming unstable.

It is recalled that in the previous relative correlation of the results an attempt was made to draw the angle of deflection into the picture. The present results show that the angle of deflection still plays an important role but no immediate relation can be established. The problem of find-

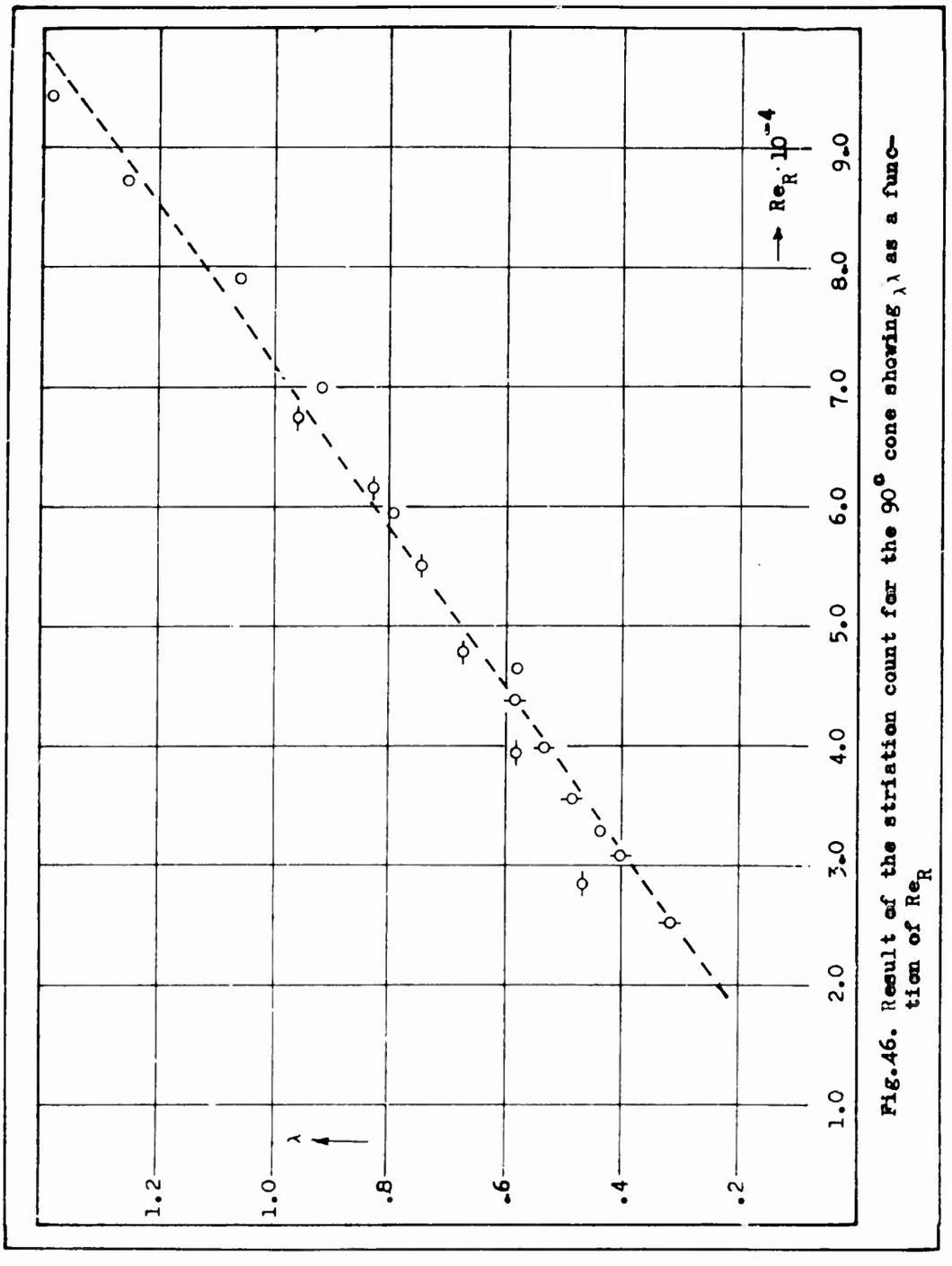

Fig.46. Result of the striation count for the 90° cone showing λ as a function of Re_R

ing the most suitable correlation whereby the reults can be utilized for flight vehicles such as reentry bodies is still being investigated and the results will be reported elsewhere.

#12. Some qualitative obsevations.

When the experiments reported on here were conducted some interesting observations were made of a qualitaive nature and it seems appropriate at this point to draw them to attention.

1) Under certain conditions the flow on the plate as well as on the cones seemed to be highly disturbed. This could be noticed as an erratical disturbance of the water surface. It was later found that this behaviour was caused by impurities in the water which had a tendency to gather in the nozzle throats for longer or shorter periods. The interesting part of this observation was however that no apparent effect of these disturbances could be noticed on the formation of the striations. It is therefore very likely that the flow responsible for the formation of the striations is confined in the laminar sublayer of the turbulent boundary layer. This is supported by numerous visual observations of the process leading to the striations. It also explains why the striations appear when the flow in the boundary layer is turbulent with presumably no regularity in it. Attention is here drawn to [4] where the dicussion of the orderly flow in the turbulent boundary layer will benefit from the introduction of the laminar sublayer. The concept presented here also makes it easy to understand why the striations observed in the original kitchen sink experiment (Fig.1) pass apparently undisturbed through the hydraulic jump.

2) In #3 attention was called to the possibility of secondary flow which might cause a long time change in the observed frequency of the striations. In #8 it was stated that no such long time effect could be found. This statement must be qualified through the following observation which also is relevant to the question of the physical mechanism responsible for the formation of the striations touched upon in #1. Close examination of the striations, especially in cases of low jet velocities when the running time needed for the striations to be fully developed was comparatively long, revealed that every second striation was "thicker" or more pronounced than those in between. It was felt that had the running time been extended, the less pronounced striations would have been completely washed away. The situation is exhibited in Fig. 47 which show a magnified picture of the stri-

ations from one of the tests. This means that if the running times of the experiments are not within certain limits the value of λ might drop by a factor of 2. Fig.47 gives however also supporting evidence to a theoretical description of the vortex system prepared by the author to be reported on elsewhere.

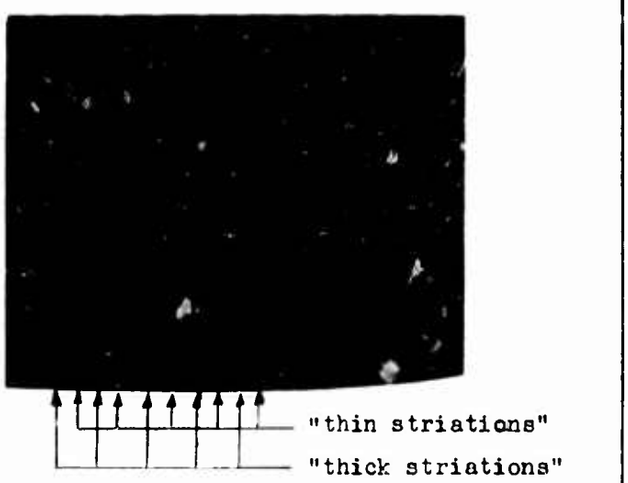

Fig.47. Magnified picture of striations showing every second striation pronounced

3) With the contention that stream-wise directed vortices are created in curved flow as a result of instability of the two-dimensional flow it follows that such vortices must be created in the nozzle and thus be present in the jet as it leaves the nozzle. In that case one is apparently faced with the problem of determining how these vortices interact with those which presumably are being created in the flow as it impinges on the model. Experimental evidence shows[1] and theoretical analysis indicates[8] that even though a region exists where the vortices are extremely stable a point is reached downstream of this region where the vortices break up. From this point downstream the flow becomes turbulent. This is indeed the case in the jet as clearly indicated by the sequence of pictures of the jet from the 1/4" nozzle shown in Fig.48. The pictures are taken at different jet speeds and the break up of the vortices is indicated by the change in the way in which the light is being reflected from the jet. For the lowest speed this does not take place within the frame of the picture. For the higher speeds it is noticed that the break-down takes place closer to the

nozzle as the speed is increased. It is also noticed that in this case the

v_o = 12.2 ft/sec v_o = 20.6 ft/sec v_o = 26.4 ft/sec

Fig.48. Break-down of vortices in th jet created in the nozzle (Arrows indicate location of nozzle opening)

distance from the nozzle to the point of break-down is of the order of 1 nozzle diameter.

The observations related above seem to make it clear that no interference between the nozzle vortices and the striations observed on the models should be present.

#13. A reentry body

Through the courtesy of the Chrysler Corporation, Missile Division, a good deal of information about their Sparta Program has been placed at the author's disposal in connection with the study of the ablation process already in progress. Although a detailed examination of this material will be reported on elsewhere, some preliminary remarks seem appropriate already at this point. One of the cone-shaped reentry vehicles in the Sparta program is shown in Fig.49 alongside a picture of the 30° cone model used

in the present investigation. The resemblance is striking. The reentry cone had a cone angle of 27.0° and the stream-wise striations formed during the ablation process give a value of $\lambda\lambda = 0.23$. This is a value that apparently

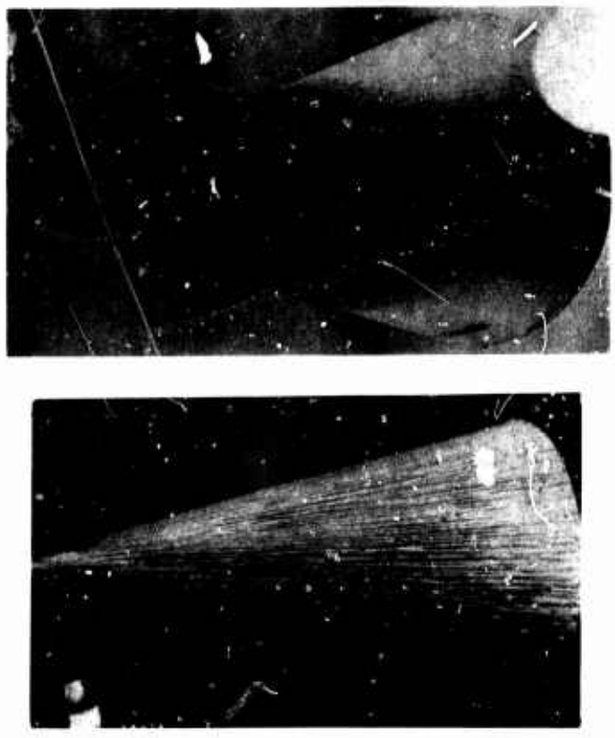

Fig.49. Recovered reentry vehicle in the Sparta program (above) compared with the 30° cone in this investigation

fits in very well with the results for the 30° cone in Fig.45. A fair comparison will however only be possible when the correlation of the present data has been properly done, and even then the comparison may be impaired by the fact that the striations in the reentry cone must have been formed in a transitional flow.

The striations on the reentry cone in Fig.49 are much better brought out by a wrapping and rubbing technique introduced at the Chrysler Corporation. Such a "rubbing" picture of the surface of the cone is shown in Fig.50. It should be noted that these "rubbings" seem to give information on the ablation process that go beyond what is presented here. This will as mentioned be taken up elsewhere.

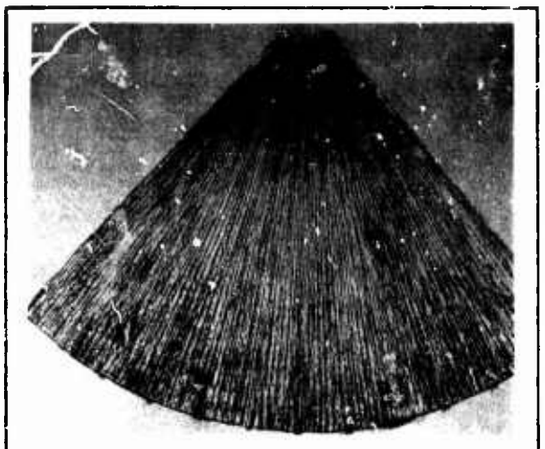

Fig.50. "Rubbing" of the surface of the reentry cone in Fig.49.

#14. Concluding remarks

Although the investigations reported on in this report are still in progress and consequently further results are expected, it is never the less felt that already at this point some definite results are established.

1) The striations ("striations" is in this report exclusively used to denote stream-wise directed lines or streaks) show such a remarkable regularity in their transverse spacing and this spacing correlates so well with the flow parameters that the following conclusion seems inescapable: The striations are indicative of a three-dimensional flow close to the surface. This three-dimensional flow may be characterized as stream-wise directed vortices. The widespread opinion that striations are "streamlines" with no other significance than to show direction of flow must be rejected. This is thought to apply also to the results of the often used "oil flow technique".

2) The stream-wise directed vortices may appear in a laminar boundary layer as well as in the laminar sublayer of a turbulent boundary layer. (It may be that under certain conditions a super-structure in the flow may be present causing hitherto unexplained patterns in the striations to occur. Such a case is among others found in the report from Douglas Aircraft Company reported on in [1]. This problem is under consideration.)

3) The striations as they appear in these experiments seem to be formed by mechanical action of the flow on the surface. (Erosion). This connects the striations closely to the shear stress at the wall and a theoretical approach to the problem is being prepared which gives a distribution of the shear stresses at the wall consistent with the appearance of the striations. In this way information is also obtained on the flow structure of the stream-wise directed vortices. (It should be mentioned that the striations found on ablating bodies may be caused by other actions than the erosion process. A detailed discussion of this point will be presented elsewhere.)

4) The contention of Dr. Max Scherberg that the stream-wise directed vortices are created as a result of the main flow becoming unstable is strongly supported. Several questions remain however to be answered. Among those are the following:

   a. What is the generally valid stability criterion?

   b. What are the general parameters characteristic of the vortex systems once they have been established?

   c. Where do the vortices start and end in space once they have been formed and the flow situation is stationary?

   In the author's opinion these are among the most important questions which must be answered before a complete picture of the physical realities behind the stream-wise directed vortices is obtained.

5) The water jet has proved itself an extremely effective and inexpensive experimental device for further investigation in the field. Indications from the present series of experiments are that an answer to 4c may be found from the water jet. These results are however at present too vague to be seriously reported on at present. Other results indicate that valuable information on the ablation process can be obtained with it.

It is noticed that throughout this report reference has been made on several occasions to future reports already in preparation. This means that the investigations are by no means brought to their conclusion.

It is however hoped that the results reported here are valuable enough to warrant this intermediate report.

#15. Acknowledgements

The author wishes to extend his sincere thanks to ARL and to Dr. Max Scherberg at ARL for the invitation to spend his sabbatical leave at ARL which made the present work possible. The author is also greatly indebted to Dr. Scherberg for his never ceasing interest and valuable suggestions in connection with these investigations. Thanks is also due to Dr. W.C. Elrod at AFIT who designed the experimental set-up and helped in the initial stages of the experiments. The courteous and expedient support of the staff and technicians of the Thermo-Mechanics Laboratories at ARL as well as that of the Me-Lab at AFIT is gratefully recognized. The courtesy of the Chrysler Corporation in placing their results at the author's disposal is deeply appreciated.

R E F E R E N C E S

[1] Leif N. Persen, "Investigation of Streamwise Vortex Systems Generated in Certain Classes of Curved Flow", Part I ARL Report 68-0134, July 1968.

[2] Murray Tobak, "Hypothesis for the Origin of Cross-Hatching", AIAA Paper No. 69-11, Jan. 1969.

[3] H.K.Larson and G.G.Mateer, "Cross-Hatching - a Coupling of Gas Dynamics with the Ablation Process", AIAA Paper No. 68-670, June 1968.

[4] T.N.Canning, M.E.Tauber, M.E.Wilkins and G.T.Chapman, "Orderly Three-Dimensional Processes in Turbulent Boundary Layers on Ablating Bodies", Report N68-34435, Ames Research Center, Moffett Field, California,

[5] H.W.Emmons, "The Laminar-Turbulent Transition in a Boundary Layer", pt.I. Jour.Aero. Sci., vol.18,July1951 pp. 490-498.

[6] A.L.Laganelli and D.E.Nestler, "Surface Ablation Patterns: A Phenomenology Study", AIAA Paper No. 68-671, June 1968.

[7] Ralph T. Wood, "An Experimental and Analytical Investigation of the Mechanism underlying the Influence of Free-Stream Turbulence on the Stagnation-Line Heat Transfer from Cylinders in Cross Flow", Thesis for the degree of Doctor of Philosophy, Div. of Eng., Brown University, June 1969.

[8] Leif N. Persen, "Investigation of Stream-wise Vortex Systems Generated in Certain Classes of Curved Flow", Part II, ARL Report 68-0133, July 1968.

Appendix I

Theoretical Background for the Re-evaluation of Data

A. 1. Introduction

The need for correlating the data with the laminar sublayer of the turbulent boundary layer makes it necessary to introduce a treatment of the turbulent boundary layer which includes the laminar sublayer. The seemingly easiest approach is then to assume a velocity distribution in the turbulent boundary layer which corresponds to the Spalding's formulation of the law of the wall [1]. The present presentation will be based on [1] and only a few general remarks will be given here. For a closer examination of the background the reader is referred to [1].

The law of the wall is defined through a universal relationship between the non-dimensional streamwise directed velocity component (u^+) and the non-dimensional distance from the wall (y^+). This relationship is formulated as

$$y^+ = u^+ + A\{e^{\kappa u^+} - 1 - \kappa u^+ - \frac{1}{2}(\kappa u^+)^2 - \frac{1}{6}(\kappa u^+)^3 - \frac{1}{24}(\kappa u^+)^4\} \qquad (1.1)$$

The non-dimensional quantities are defined through the shear-velocity v_* defined by

$$\tau_w = \rho v_*^2 \qquad (1.2)$$

where τ_w is the shear stress at the wall.

In the present case of an axis-symmetric jet hitting the wall at right angle, the flow will be described in a cylindrical coordinate system as shown in Fig. A. 1.

The non-dimensional velocity u^+ is now defined as

$$u^+ = \frac{v_r}{v_*} \qquad (1.3)$$

and the non-dimensional wall distance is

$$y^+ = \frac{zv_*}{\nu} \tag{1.4}$$

It will be assumed that the law of the wall (1.1) applies to the boundary layer that develops along the wall. It is thereby observed that at a sufficiently large distance from the stagnation point the boundary layer thickness h is equal to the thickness of the water film.

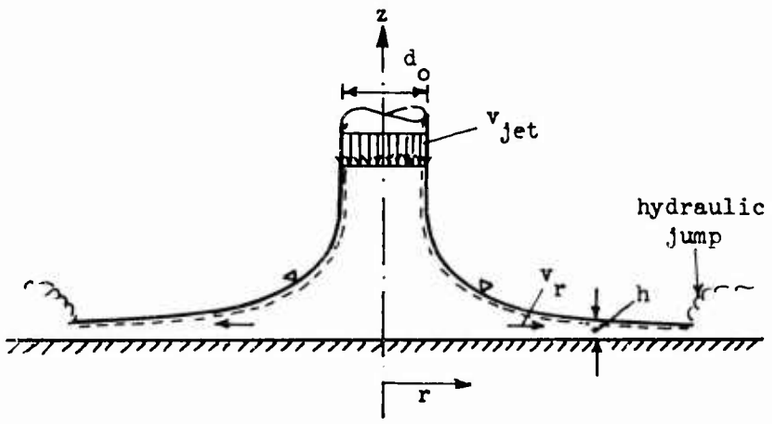

Fig. A1. Sketch of water jet impinging on a flat plate with the coordinate system.

A. 2. The equation of continuity.

The equation of continuity may take different forms as will be shown later. At the present time the attention is fixed at the overall condition which for a given experiment where the discharge q_o is given, may take the following form

$$q_o = \int_o^h v_r \cdot 2\pi r dz \tag{2.1}$$

Because of the non-dimensional description which is introduced, this equation may be rewritten as

$$q_o = \int_o^h u^+(y^+) \cdot 2\pi r v_*(r) dz \tag{2.2}$$

The value of y^+ at z = h will be denoted y_o^+ and in consequence of (1.1) $u^+(y_o^+)$ which is denoted ξ, will be related to y_o^+ as follows

$$y_o^+ = \xi + A\{e^{\kappa\xi} - 1 - \kappa\xi - \frac{1}{2}(\kappa\xi)^2 - \frac{1}{6}(\kappa\xi)^3 - \frac{1}{24}(\kappa\xi)^4\} \qquad (2.3)$$

where

$$y_o^+ = \frac{hv_*}{\nu} \qquad \xi = \frac{v_{r.o}}{v_*} \qquad (2.4)$$

$v_{r.o}$ = radial velocity at the surface of the water film

Through introduction of the diameter of the water jet the jet velocity v_{jet} is defined as

$$v_{jet} = \frac{4q_o}{\pi d_o^2}$$

and the Reynolds' number R_{jet} of the jet will be

$$Re_{jet} = \frac{v_{jet}\, d_o}{\nu} = \frac{4q_o}{\pi\, d_o \nu} \qquad (2.5)$$

This means that (2.2) may be reformulated as

$$\frac{1}{4}Re_{jet} \cdot \frac{r_o}{r} = \int_o^{y_o^+} u^+(y^+)dy^+ = \int_o^{\xi} u^+ \frac{dy^+}{du^+}\, du^+ = L(\xi) \qquad (2.6)$$

where $L(\xi)$ is defined as in [1] and given explicitly as

$$L(\xi) = \frac{1}{2}\xi^2 + \frac{A}{\kappa}\{e^{\kappa\xi}(\kappa\xi-1) + 1 - \frac{1}{2}(\kappa\xi)^2 - \frac{1}{3}(\kappa\xi)^3 - \frac{1}{8}(\kappa\xi)^4 - \frac{1}{30}(\kappa\xi)^5\} \qquad (2.7)$$

The non-dimensional radial coordinate ζ is defined as

$$\zeta = \frac{r}{r_o} \qquad (2.8)$$

where r_o is the radius of the jet($=d_o/2$) and the continuity equation is finally brought into the form:

$$\zeta = \frac{1}{4}Re_{jet}/L(\xi) \qquad (2.9)$$

This equation determines the value of ξ at each radial location, and thereby (through (2.3)) the value of y_o^+ is known at the same location. It means that the non-dimensional film thickness y_o^+ is now known implicitly as a function of $r/r_o = \zeta$ but v_* remains unknown. Therefore the dimensional thickness still remains unknown.

Before proceeding to a consideration of the momentum equation, it should perhaps be noted that (2.9) carries in it some important consequences. Because ξ decreases with increasing radial distance (ζ increasing) it is clear that the laminar sublayer will be an increasing portion of the total film thickness. This feature of the solution is just in line with what is to be expected and renders credibility to the approach.

Inherent in the approach is also the similarity of the configuration of two different jets if their Reynolds' numbers are the same. Also this feature of the approach seems to be reasonable. (See additional remarks, section #9)

A. 3. The momentum equation.

The lacking information is now to be obtained from the momentum equation. This may be obtained by considering an element of the water film as sketched in Fig. A2. The pressure may be assumed to be statically distributed due to the

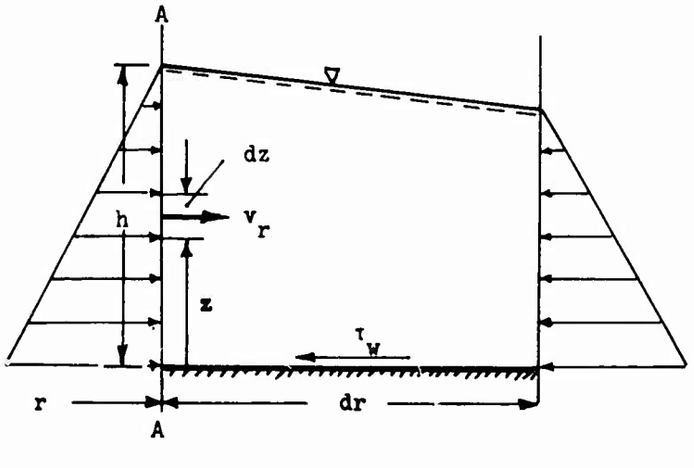

Fig. A2. Sketch of an element of the water film.

free water surface. Thus the total pressure P on the section A-A may be written

$$P = \int_0^h \gamma(h-z)dzrd\phi = \gamma r \frac{h^2}{2} d\phi \tag{3.1}$$

The total force acting or the element in the positive r-direction will then be

$$-\tau_w rd\phi dr - \frac{\partial}{\partial r} \{\gamma r \frac{h^2}{2} d\phi\}dr \tag{3.2}$$

whereby the component of the atmospheric pressure acting on the free surface has been neglected as well as the shear stress at the same surface.

The momentum transport B through A-A will be

$$B = \int_0^h \rho v_r^2 \, rd\phi \, dz \tag{3.3}$$

For the entire element one thus has the change per unit time of momentum equated to the force acting on it, which leaves

$$-\tau_w rd\phi dr - \frac{\partial}{\partial r} [\gamma r \frac{h^2}{2} d\phi]dr = + \frac{\partial}{\partial r} \{ \int_0^h \rho v_r^2 \, rd\phi dz\}dr$$

or

$$- \frac{\partial}{\partial r} \{r \int_0^h \rho v_r^2 \, dz\} = \frac{\partial}{\partial r} \{\rho r \frac{h^2}{2}\} + r\tau_w \tag{3.4}$$

Now the law of the wall is drawn to attention: [redacted]

$$\int_0^h v_r^2 dz = \int_0^h (u^+)^2 v_*^2 \, dz = \nu v_* \int_0^{y_o^+} (u^+)^2 dy^+ = \nu v_* \int_0^{\xi} (u^+)^2 \frac{dy^+}{du^+} du^+ = \nu v_* G(\xi) \tag{3.5}$$

where $G(\xi)$ is defined in [1] and may explicitly be written:

$$G(\xi) = \frac{1}{3}\xi^3 + \frac{A}{\kappa^2}[e^{\kappa\xi}\{(\kappa\xi)^2 - 2(\kappa\xi) + 2\} - 2 - \frac{1}{3}(\kappa\xi)^3 - \frac{1}{4}(\kappa\xi)^4 - \frac{1}{10}(\kappa\xi)^5 - \frac{1}{36}(\kappa\xi)^6] \tag{3.6}$$

The momentum equation (3.4) may now be reformulated as

$$- \frac{\partial}{\partial r}[\nu r v_* G(\xi)] = g \frac{\partial}{\partial r}[r \frac{h^2}{2}] + r v_*^2 \tag{3.7}$$

Now, in the region of interest the pressure term is not significant and may be neglected, leaving

$$- \frac{\partial}{\partial r} [\nu r v_* G(\xi)] = r v_*^2 \tag{3.8}$$

At this point it is now useful to introduce the following non-dimensional quantities:

$$\begin{aligned} &\text{Non-dimensional radial distance:} && \zeta = \frac{r}{r_o} \\ &\text{Non-dimensional water film thickness:} && \delta = \frac{h}{r_o} \end{aligned} \tag{3.9}$$

Because of the definition of y_o^+ in (2.4) the shear velocity may be expressed as

$$v_* = \frac{\nu}{r_o} \frac{y_o^+(\xi)}{\delta} \tag{3.10}$$

So, introduced into (3.8) this gives:

$$- \frac{1}{\zeta} \frac{\partial}{\partial \zeta} [\zeta \frac{y_o^+}{\delta} G(\xi)] = - \frac{[y_o^+(\xi)]^2}{\delta^2} \tag{3.11}$$

Because of the continuity equation (2.9) ξ may be considered a known function of ζ and (3.11) will then give δ as a function of ζ, i.e. the wanted information. However, if ζ is thought of as a function of ξ [through (2.9)] then (3.11) will render δ as a function of ξ. This method of approach will be used here.

From (2.9) one obtains:

$$\frac{d\xi}{d\zeta} = - \frac{1}{\zeta} \frac{L(\xi)}{L'(\xi)} \tag{3.12}$$

and (3.11) may after some rearrangements be brought in the form

$$\boxed{\frac{d}{d\xi} \left[\frac{\delta \, L(\xi)}{\frac{1}{4} Re_{jet} \, y_o^+(\xi) \, G(\xi)} \right] = - \frac{L'(\xi)}{L(\xi)[C(\xi)]^2}} \tag{3.13}$$

Before proceeding to solve this equation, the entire background of the equation may perhaps be reconsidered in terms of the Navier-Stokes' equations. For the present case these may be given as

$$v_r \frac{\partial v_r}{\partial r} + v_z \frac{\partial v_r}{\partial z} = + \frac{1}{\rho} F_r - \frac{1}{\rho} \frac{\partial p}{\partial r} + \frac{1}{\rho} \left(\frac{\partial \sigma_r}{\partial r} + \frac{\sigma_r}{r} + \frac{\partial \tau_{rz}}{\partial z} \right)$$

$$v_r \frac{\partial v_z}{\partial r} + v_z \frac{\partial v_z}{\partial z} = + \frac{1}{\rho} F_z - \frac{1}{\rho} \frac{\partial p}{\partial z} + \frac{1}{\rho} \left(\frac{\partial \sigma_z}{\partial z} + \frac{\tau_{rz}}{r} + \frac{\partial \tau_{rz}}{\partial z} \right) \qquad (3.14)$$

where the "viscous" terms have been expressed in terms of the stress components and where F_r and F_z represent the components of the body force. In addition to these equations the continuity equation enters in the form

$$\frac{\partial}{\partial r} (r v_r) + \frac{\partial}{\partial z} (r v_z) = o \qquad (3.15)$$

Now, because the flow to be studied has a free surface, the main terms in the second equation (3.14) will be the pressure term and the body force, i.e.

$$o = \frac{1}{\rho} F_z - \frac{1}{\rho} \frac{\partial p}{\partial z} \qquad (3.16)$$

The body force is created by the gravitational field which in the present case gives:

$$F_r = o, \; F_z = - \gamma, \; \frac{\partial p}{\partial z} = - \gamma, \; p = \gamma (h - z) \qquad (3.17)$$

Next the influence of σ_r is neglected and the first equation (3.14) becomes

$$v_r \frac{\partial v_r}{\partial r} + v_z \frac{\partial v_r}{\partial z} = - g \frac{\partial h}{\partial r} + \frac{1}{\rho} \frac{\partial \tau_{rz}}{\partial z} \qquad (3.18)$$

The continuity equation suggests the introduction of a stream-function Ψ as follows:

$$\frac{\partial \Psi}{\partial r} = - r v_z, \; \frac{\partial \Psi}{\partial z} = r v_z \qquad (3.19)$$

The law of the wall now makes the following representation of Ψ possible:

$$\Psi = \int_o^z r v_r dz = r \int_o^z u^+ v_* dz = \nu r \int_o^{y^+} u^+ dy^+ \qquad (3.20)$$

and v_z may be deduced as

$$- v_z \cdot r = \frac{\partial}{\partial r} \{ \int_o^{y^+} u^+ dy^+ \cdot r\nu \} = \nu \int_o^{y^+} u^+ dy^+ + r \frac{\nu}{v_*} \frac{dv_*}{dr} u^+ y^+ \qquad (3.21)$$

The procedure by means of which the equation (3.18) is now brought in its final form follows the same lines as in [1] and the result will be:

$$(u^+)^2 v_* \frac{dv_*}{dr} - \frac{v_*^2}{r} \frac{du^+}{dy^+} \int_o^{y^+} u^+ dy^+ = - g \frac{dh}{dr} + \frac{v_*}{\rho\nu} \frac{\partial \tau_{rz}}{\partial y^+} \qquad (3.22)$$

In this equation the appearing functions are either functions of r only or of y^+ only except τ_{rz} which now is assumed to depend on both y^+ and r. Thus a formal integration is possible with respect to y^+:

$$v_* \frac{dv_*}{dr} \int_o^{y_o^+} (u^+)^2 dy^+ - \frac{v_*}{r} \int_o^{y_o^+} \frac{du^+}{dy^+} \{ \int_o^{y^+} u^+ dy^+ \} dy^+ = - g y_o^+ \frac{dh}{dr} - \frac{v_*}{\nu\rho} \rho v_*^2 \qquad (3.23)$$

Here the definition of v_* (1.2) has been drawn to attention and the shear stress at the free surface has been neglected. Partial integration and neglection of the pressure term finally converts (3.23) into

$$\nu \left(\frac{dv_*}{dr} + \frac{v_*}{r} \right) G(\xi) - \nu \frac{v_*}{r} \xi L(\xi) = - v_*^2 \qquad (3.24)$$

Introduction of the non-dimensional quantities (3.9) and replacement of v_* by δ through (3.10) leads to

$$\frac{1}{\zeta} \frac{d}{d\zeta} \left[\zeta \frac{y_o^+}{\delta} \right] G(\xi) - \frac{1}{\zeta} \frac{y_o^+}{\delta} \xi L(\xi) = - \left(\frac{y_o^+}{\delta} \right)^2 \qquad (3.25)$$

Again the transformation to ξ as the independent variable will give

$$\boxed{\frac{d}{d\xi} \left[\frac{L(\xi)\delta}{\frac{1}{4} Re_{jet} y_o^+} \right] G(\xi) - \frac{L(\xi)}{\frac{1}{4} Re_{jet} y_o^+} \frac{dG}{d\xi} = - \frac{L'(\xi)}{L(\xi)}} \qquad (3.26)$$

In addition to (3.12) the following relations obtained from the definitions of the functions $L(\xi)$ and $G(\xi)$ have been used to bring about the transformation

$$L(\xi) = \int_0^{\xi} u^+ \frac{dy^+}{du^+}\, du^+, \quad G(\xi) = \int_0^{\xi} (u^+)^2 \frac{dy^+}{du^+}\, du^+, \quad \frac{dG}{d\xi} = \xi \frac{dL}{d\xi} = \xi L'(\xi) \qquad (3.27)$$

It is a matter of routine algebra to show that (3.26) is identical to (3.13).

Before proceeding to the solution of the momentum equation a special point should be stressed. The equation has been deduced on the basic assumption that the static pressure term can be neglected. This means that one can only apply the solution to the annular region on the plate where the jet has spread out to form a film.

A. 4. The solution to the momentum equation.

The deduction of the solution to (3.26) [or (3.13)] is very simple because it can be obtained through a simple integration. Formally, therefore, the solution may be put in the form:

$$\frac{\delta L(\xi)}{\frac{1}{4} \mathrm{Re}_{jet}\, y_o^+(\xi) G(\xi)} = C_o - \int_{\xi_o}^{\xi} \frac{L'(\xi) d}{L(\xi)[G(\xi)]^2} \qquad (4.1)$$

where C_o is a constant of integration. It is the determination of this constant that may be problematic.

It is remembered from (2.9) that small values of ξ correspond to larger values of ζ. Because of the hydraulic jump [Fig. A.1] it is clear that the present solution only applies to values of ζ less that ζ_j (the value of ζ at the jump). For reasons mentioned above, the lower bound of ζ will be estimated at 4. Thus the solution will be limited to the region

$$4 \leq \zeta \leq \zeta_j \qquad (4.2)$$

or to the region where the striations occur. This further makes it natural to consider the position $\zeta = \zeta_j$ as the point where a condition determining the value of C_o will have to be introduced. At this location, therefore, ξ may be expected to be small, and the solution for small values of ξ becomes important.

Now, for small values of ξ, i.e., for $\xi \leq 5$, the following simplified expressions are valid to within 1% accuracy:

$$y_o^+(\xi) \doteq \xi, \; G(\xi) \doteq \frac{1}{3}\xi^3, \; L(\xi) \doteq \frac{1}{2}\xi^2 \tag{4.3}$$

Introduced into (4.1) this gives:

$$\delta = \frac{1}{2} Re_{jet} \left(\frac{1}{3} C_o - \xi_j^{-6} \right) \xi^2 + \frac{1}{2} Re_{jet} \cdot \xi^{-4} \tag{4.4}$$

where ξ_j corresponds to ζ_j.

Now it is clear that because ξ increases with decreasing values of ζ the values of δ must increase with increasing values of ξ. Eq. (4.4) then indicates that the solution to the homogeneous equation (3.26) will be the predominant term of the solution in the region of interest. This means that the integral in (4.1) can be neglected and consequently

$$\delta = C_o \cdot \frac{1}{4} Re_{jet} \frac{y_o^+(\xi) G(\xi)}{L(\xi)} \tag{4.5}$$

where C_o will have to be determined from conditions at $\zeta = \zeta_j$.

For the re-evaluation of the data the thickness h_s of the laminar sublayer is to be drawn to attention. This thickness will here be given non-dimensionally through δ_s whereby:

$$\delta_s = \frac{h_s}{r_o} = \frac{h_s}{h} \cdot \frac{h}{r_o} = \frac{h_s}{h} \delta \tag{4.6}$$

The ratio h_s/h is defined by interpreting the value of $y_o^+(5)$ as the non-dimensional thickness of the laminar sublayer for each value of ξ, thus:

$$\frac{h_s}{h} = \frac{h_s v_*}{\nu} \Big/ \frac{h v_*}{\nu} = \frac{y_o^+(5)}{y_o^+(\xi)} \tag{4.7}$$

Gathering these results one obtains:

$$\delta_s = C_o \frac{1}{4} Re_{jet} \frac{G(\xi)}{L(\xi)} \tag{4.8}$$

Table AI

ξ	$\zeta = r/r_o$	$\delta_s = h_s/r_o$		ξ	$\zeta = r/r_o$	$\delta_s = h_s/r_o$
14.9	4.9384309E+01	7.1019697E+00		17.6	1.4037148E+01	8.7466883E+00
15.0	4.7176625E+01	7.1645038E+00		17.7	1.3392748E+01	8.8058790E+00
15.1	4.5062780E+01	7.2269291E+00		17.8	1.2777951E+01	8.8649599E+00
15.2	4.3039273E+01	7.2892388E+00		17.9	1.2191424E+01	8.9239338E+00
15.3	4.1102679E+01	7.3514302E+00		18.0	1.1631888E+01	8.9828041E+00
15.4	3.9249673E+01	7.4135009E+00		18.1	1.1098121E+01	9.0514714E+00
15.5	3.7477017E+01	7.4754492E+00		18.2	1.0588953E+01	9.1002398E+00
15.6	3.5781567E+01	7.5372697E+00		18.3	1.0103263E+01	9.1588106E+00
15.7	3.4160271E+01	7.5989640E+00		18.4	9.6399810E+00	9.2172873E+00
15.8	3.2610171E+01	7.6605285E+00		18.5	9.1980801E+00	9.2756701E+00
15.9	3.1128396E+01	7.7219634E+00		18.6	8.7765807E+00	9.3339626E+00
16.0	2.9712175E+01	7.7832681E+00		18.7	8.3745500E+00	9.3921699E+00
16.1	2.8358815E+01	7.8444400E+00		18.8	7.9910903E+00	9.4502900E+00
16.2	2.7065725E+01	7.9054822E+00		18.9	7.6253461E+00	9.5083287E+00
16.3	2.5830392E+01	7.9663912E+00		19.0	7.2765025E+00	9.5662876E+00
16.4	2.4650400E+01	8.0271704E+00		19.1	6.9437757E+00	9.6241659E+00
16.5	2.3523411E+01	8.0878193E+00		19.2	6.6264253E+00	9.6819687E+00
16.6	2.2447170E+01	8.1483380E+00		19.3	6.3237379E+00	9.7397002E+00
16.7	2.1419514E+01	8.2087276E+00		19.4	6.0350328E+00	9.7973601E+00
16.8	2.0438348E+01	8.2689907E+00		19.5	5.7596663E+00	9.8549516E+00
16.9	1.9501663E+01	8.3291261E+00		19.6	5.4970153E+00	9.9124733E+00
17.0	1.8607530E+01	8.3891390E+00		19.7	5.2464920E+00	9.9699326E+00
17.1	1.7754085E+01	8.4490265E+00		19.8	5.0075326E+00	1.0027327E+01
17.2	1.6939545E+01	8.5087936E+00		19.9	4.7796000E+00	1.0084664E+01
17.3	1.6162198E+01	8.5684423E+00		20.0	4.5621819E+00	1.0141940E+01
17.4	1.5420389E+01	8.6279726E+00		20.1	4.3547890E+00	1.0199160E+01
17.5	1.4712545E+01	8.6873870E+00		20.2	4.1569555E+00	1.0256329E+01
				20.3	3.9682363E+00	1.0313442E+01

In Table AI corresponding values of ξ, ζ and δ_s have been tabulated for $Re_{jet} = 50{,}000$. Hereby C_o has been arbitrarily chosen which, however, only shows up as a constant factor in δ_s and thus does not invalidate the subsequent conclusions.

The range of variation for ξ and ζ on the test plate is obtained from the size of the test plate, of the jet diameter and from Table AI. The result is shown with approximate values in Table AII. (valid only for $Re_{jet} = 50{,}000$)

Table AII

Nozzle	ζ_{min}	corresp. ξ_{max}	corresp. $\delta_{s\ max}$	ζ_{max}	corresp. ξ_{min}	corresp. $\delta_{s\ min}$
1/8"	4.0	20.2	10.26	48	15.0	7.16
1/4"	4.0	20.2	10.26	24	16.5	8.09
3/8"	4.0	20.2	10.26	16	17.3	8.57

From this table one gets a good idea of the variation of the thickness of the laminar sublayer which can be expected in these measurements. It is once again stressed that the values given are only relative because the constant C_o of integration has not been determined. This must be done by drawing suitable experimental results into consideration.

REFERENCE

(1) Ronald S. Brand, Leif N. Persen — "Implications of the Law of the Wall for Turbulent Boundary Layers," Acta Polytechnica Scandinavica Ph 30, (1964).

Appendix II

"Best fit" procedure through least mean squares.

Assume that one has a series of measured data which are suspected of defining a straight line when the measured values y_i are plotted as a function of the measured values x_i. The straight line is defined through

$$y = ax + b \tag{1.1}$$

The deviation v_i of the measured values are then defined as:

$$v_i = y_i - ax_i - b \tag{1.2}$$

Assume further that the measured values are obtained from different nozzles and that a fair comparison can only be obtained if x_i from the 1/4" nozzle is multiplied by c_2 and x_i from the 1/8" nozzle is multiplied by c_1. One would then have 3 types of deviations:

$$\begin{aligned} &\text{3/8" nozzle:} \quad v_i^{(3)} = y_i - ax_i - b \\ &\text{2/8" nozzle:} \quad v_i^{(2)} = y_i - ac_2x_i - b \\ &\text{1/8" nozzle:} \quad v_i^{(1)} = y_i - ac_1x_i - b \end{aligned} \tag{1.3}$$

The sum of the squares of all deviations S would be:

$$S = \Sigma_1(v_i^{(1)})^2 + \Sigma_2(v_i^{(2)})^2 + \Sigma_3(v_i^{(3)})^2 \tag{1.4}$$

The "best fit" method through the least mean squares then requires:

$$\frac{\partial S}{\partial a} = 0,\ \frac{\partial S}{\partial b} = 0,\ \frac{\partial S}{\partial c_2} = 0 \text{ and } \frac{\partial S}{\partial c_1} = 0 \qquad (1.5)$$

This gives 4 equations for the 4 unknown quantities a, b, c_1 and c_2. It will be assumed that there are n_1, n_2 and n_3 measurements for the 1/8", the 2/8" and the 3/8" nozzle respectively. The total number of measurements are $n_1 + n_2 + n_3 = n$. The set of equations from (1.5) may then be written as follows:

$$\begin{aligned}
b\cdot\Sigma_3 x_i + a\cdot\Sigma_3 x_i^2 &= +\Sigma_3 x_i y_i \\
b\,\Sigma_2 x_i + ac_2\cdot\Sigma_2 x_i^2 &= +\Sigma_2 x_i y_i \\
b\,\Sigma_1 x_i + ac_1\cdot\Sigma_1 x_i^2 &= +\Sigma_1 x_i y_i \\
b\cdot n + a\Sigma_3 x_i + ac_2\Sigma_2 x_i + ac_i\cdot\Sigma_1 x_i &= +\Sigma\ y_i
\end{aligned} \qquad (1.6)$$

where Σ_i denotes summation over values obtained with i/8" nozzle and Σ denotes summation over all values from all nozzles.

This linear set of equations can easily be solved.

UNCLASSIFIED
Security Classification

DOCUMENT CONTROL DATA - R & D

(Security classification of title, body of abstract and indexing annotation must be entered when the overall report is classified)

1. ORIGINATING ACTIVITY *(Corporate author)*
Institutt for Mekanikk
Trondheim, Norway

2a. REPORT SECURITY CLASSIFICATION
UNCLASSIFIED

2b. GROUP

3. REPORT TITLE
Exploratory Experiments In Water On Stream-Wise Directed Vortices And Crosshatching Of The Surface Of Reentry Bodies

4. DESCRIPTIVE NOTES *(Type of report and inclusive dates)*
Scientific. Final.

5. AUTHOR(S) *(First name, middle initial, last name)*
Professor Lief N. Persen

6. REPORT DATE	7a. TOTAL NO. OF PAGES	7b. NO. OF REFS
September 1969	76	8

8a. CONTRACT OR GRANT NO.	9a. ORIGINATOR'S REPORT NUMBER(S)
F33615-67-C-1758	
b. PROJECT NO. 7063	
c. DoD Element 61102F	9b. OTHER REPORT NO(S) *(Any other numbers that may be assigned this report)*
d. DoD Sub-Element 681307	ARL 69-0160

10. DISTRIBUTION STATEMENT
1. This document has been approved for public release and sale; its distribution is unlimited.

11. SUPPLEMENTARY NOTES	12. SPONSORING MILITARY ACTIVITY
TECH OTHER	ARL (ARN) WPAFB, Ohio 45433

13. ABSTRACT

Contained in this report is a detailed description of the experimental results obtained on the stream-wise vortices using a water jet as an experimental device. Information on the vortices were obtained through a study of the stream-wise striations left in the coat on the models used by the outside flow. Striation counts were performed and the "wavenumber" thus obtained is related to the flow parameters. The contention that the stream-wise vortices appear as a result of the outside curved flow becoming unstable is strongly supported. The investigation is not finished and further work has already been undertaken.

DD FORM 1 NOV 65 1473

UNCLASSIFIED
Security Classification

14 KEY WORDS	LINK A		LINK B		LINK C	
	ROLE	WT	ROLE	WT	ROLE	WT
Stream-Wise Vortices						
Water Jet						
Wavenumber						
Flow Parameters						